CONFIDENTIAL

Copy
RM L57

16256
AUG 13 1957

TECH LIBRARY KAFB, NM
0144797

NACA RM L57F05

7782

NACA

RESEARCH MEMORANDUM

TWO-DIMENSIONAL AIRFOIL CHARACTERISTICS OF FOUR NACA 6A-SERIES AIRFOILS AT TRANSONIC MACH NUMBERS UP TO 1.25

By Charles L. Ladson

Langley Aeronautical Laboratory
Langley Field, Va.

CLASSIFIED DOCUMENT

This material contains information affecting the National Defense of the United States within the meaning of the espionage laws, Title 18, U.S.C., Secs. 793 and 794, the transmission or revelation of which in any manner to an unauthorized person is prohibited by law.

NATIONAL ADVISORY COMMITTEE
FOR AERONAUTICS

WASHINGTON
August 6, 1957

CONFIDENTIAL

[redacted]

TECH LIBRARY KAFB, NM
0144797

NATIONAL ADVISORY COMMITTEE FOR AERONAUTICS

RESEARCH MEMORANDUM

TWO-DIMENSIONAL AIRFOIL CHARACTERISTICS OF FOUR NACA 6A-SERIES AIRFOILS AT TRANSONIC MACH NUMBERS UP TO 1.25

By Charles L. Ladson

SUMMARY

A two-dimensional wind-tunnel investigation of the flow and force characteristics of four NACA 6A-series airfoils with thickness ratios of 4, 6, and 9 percent has been conducted in the Langley airfoil test apparatus at transonic Mach numbers between 0.8 and 1.25. The Reynolds number range for these tests varied from 2.6×10^6 to 2.8×10^6.

As was expected, the airfoils exhibited a smooth transition in force coefficients from a Mach number of 1.0 to the values obtained at the higher speeds. Lift-curve slope and maximum lift-drag ratio correlated very well on a basis of the transonic similarity laws at Mach numbers above 1.0, but below that value the correlation was not good. The measured effect of thickness on the drag coefficient at supersonic speeds was less than that predicted by the transonic similarity laws. Good correlation of the drag coefficients was obtained by reducing the exponent of the thickness term from the theoretical value of 1.67 to 1.50. This change did not affect the correlation at subsonic speeds, which was good for either case.

INTRODUCTION

Two-dimensional airfoil data at subsonic and transonic speeds are used not only in wing design and the prediction of propeller performance, but also are an important source of basic information of the flow and force variations of different airfoil sections. By means of pressure distributions, force coefficients, and schlieren photographs, the effects of variables such as thickness, thickness distribution, and camber may be studied independently. Available information of this type has been limited generally to Mach numbers below 1.0 inasmuch as most data were obtained in closed-throat tunnels which limited the speed range of the tests to Mach numbers below the choking value. The Langley 4- by

UNCLASSIFIED

[redacted]

19-inch semiopen tunnel (ref. 1) enabled data to be obtained up to and including a Mach number of 1.0. Considerable interest, however, has been shown in obtaining two-dimensional data throughout the transonic speed range and into the low supersonic regime. Although some scattered two-dimensional data are available at low supersonic Mach numbers (for example, see refs. 2 and 3), the data are limited.

A new facility, designated the Langley airfoil test apparatus (ATA), has therefore been constructed and placed in operation at the Langley Laboratory. This facility has a 4- by 19-inch slotted test section and is capable in its present arrangement of operation at Mach numbers from subsonic values up to a maximum Mach number of 1.25. At the maximum Mach number, the Reynolds number may be varied from about 2×10^6 to 7×10^6, based on a 4-inch-chord model through control of the stagnation pressure. A complete description of the ATA and a comparison with results obtained in other facilities are presented.

The present investigation was made on four NACA 6A-series airfoils of thicknesses of 4 to 9 percent over a Mach number range from 0.8 to 1.25. The corresponding Reynolds number of the 4-inch-chord models tested at a stagnation pressure of 26 pounds per square inch absolute varied from 2.6×10^6 to 2.8×10^6. The models were all symmetrical and were tested at angles of attack from 0° to 8°. Pressure distributions and schlieren flow photographs of the models were obtained. The basic force data are presented and are compared at Mach numbers above 1.0 with supersonic theory.

SYMBOLS

c	airfoil chord
c_d	section drag coefficient
$c_{d,o}$	section drag coefficient at zero lift
$c_{d,p}$	section pressure drag coefficient
c_l	section lift coefficient
c_n	section normal-force coefficient
$c_{m,c/4}$	section moment coefficient about quarter chord
c_{l_α}	section lift-curve slope, $\partial c_l/\partial \alpha$
p_t	stagnation pressure, lb/sq in. abs

M	test-section Mach number
l/d_p	section lift-drag ratio
$\left(l/d_p\right)_{max}$	maximum section lift-drag ratio
t	airfoil maximum thickness
x_{cp}	location of center of pressure
α	angle of attack, deg
ξ	reduced Mach number (transonic similarity parameter)

APPARATUS

General Description of Apparatus

The tests were conducted in the Langley airfoil test apparatus (ATA) which is a two-dimensional slotted-throat facility operating on direct blowdown from a supply of dry compressed air. (See fig. 1(a).) The facility incorporates mechanical features which permit independent control of both stagnation pressure and free-stream Mach number. The settling-chamber stagnation pressure is controlled by a pneumatic pressure-regulating valve which enables tests to be made at any constant stagnation pressure from 26 to 60 pounds per square inch absolute.

Air enters the 4- by 19-inch slotted test section through a sonic nozzle from a circular settling chamber of about 5 feet in diameter. The area contraction ratio from settling chamber to test section is about 45:1. Three longitudinal slots are located in each of the 4-inch-wide walls, the slots having a total width of 1/2 inch or 1/8 open area. As seen in figure 1(a), the slots begin (at tunnel station 45) 25 inches upstream of the test-region center line and extend slightly downstream of the test region. Figure 1(b) presents a more detailed sketch of the test section, showing the plenum chamber which surrounds the 4- by 19-inch test region. Ducts (see fig. 1(b)) of 62-square-inch cross section connect the plenum chamber adjacent to the slotted walls to eliminate any pressure differentials which may have existed. Air which has passed through the slots into the plenum chamber is returned to the main airstream over reentrant flow fairings downstream of the test section. The minimum area in this mixing section ahead of the chokers is 20 percent larger than the test-section area to provide space for low-energy reentrant flow to return to the main stream. Tunnel calibrations showed that the 20-percent increase in area limited the maximum test Mach number to 1.25.

A choker section located downstream of the mixing region (from tunnel station 98 to 120) is used to control the Mach number. The two 19-inch-high sidewalls are made of thin flexible metal, so that they may be deflected into the airstream. When deflected, these walls decrease the cross-sectional area, thus decreasing the tunnel mass flow. Since sonic speed was maintained at the choker minimum area, the test-section Mach number could be set at any value, depending upon the amount of deflection of the flexible walls.

A transition section is located downstream of the choker section and followed by a conical diffuser which exhausts the tunnel to the atmosphere.

Mach Number Distribution in Test Section

Static-pressure measurements were made for the tunnel-empty condition to determine the Mach number distribution in both streamwise and normal-to-stream directions. Figure 2 shows the streamwise Mach number distribution for test Mach numbers from 0.4 to 1.25. The data presented were obtained by varying the stagnation pressure with the choker wide open. Other calibrations were made at various constant stagnation pressures by using the choker to vary the Mach number. These data showed no change in the Mach number gradients from those presented in figure 2 and are therefore not presented.

An examination of the data shows the Mach number variation from 1 chord length ahead to 1 chord length behind the center of the test region (station 70) to be about ±0.002. A similar examination of the Mach number gradients in the normal-to-stream direction (taken at tunnel station 70) shows a maximum variation of ±0.010 from 1 chord above to 1 chord length below the model chord line.

MODELS

The models tested in this investigation were the NACA 65A004, 65A006, 65A009, and 64A006 airfoil sections. Ordinates for the NACA 65A-series are given in reference 4 and for the NACA 64A006 section in reference 1. All models were of 4-inch chord and completely spanned the 4-inch width of the tunnel. Static-pressure orifices having diameters of 0.0135 inch were drilled normal to the airfoil surface and were located on both upper and lower surfaces near the midspan section. All models had orifices located at the 2.5-, 5.0-, 7.5-, 10-, 15-, 20-, 25-, 30-, 35-, 40-, 45-, 50-, 55-, 60-, 65-, 70-, 75-, 80-, 85-, and 90-percent-chord stations; the NACA 65A009 also had orifices at the 1.25- and 95-percent-chord stations.

TESTS

Methods and Range

The orifices in the model were connected to both a multitube manometer board and an NACA electrical pressure integrator. By means of this setup simultaneous pressure distributions and integrated normal force and moment were recorded. Pressure distributions were plotted normal to the model thickness and were integrated to obtain chord forces. From these data, the lift, drag, and moment coefficients presented herein were computed. Schlieren motion pictures of the flow past the models were obtained during separate tests, and representative frames have been presented. The exposure time of each frame is approximately 4 microseconds.

The tests covered a Mach number range from 0.8 to 1.25, an angle-of-attack range from 0° to 8°, and a Reynolds number range of 2.6×10^{6} to 2.8×10^{6}. The stagnation pressure was held constant throughout the tests at 26 pounds per square inch absolute.

Comparison With Other Data

Although little two-dimensional data exist for Mach numbers above 1.0 to compare with the ATA data, a comparison at lower Mach numbers is made with data from the Langley 4- by 19-inch semiopen tunnel (ref. 1). This two-dimensional open-throat tunnel was capable of attaining a maximum Mach number of 1.0 and operated on atmospheric air induced to flow through the test section by an induction nozzle. Since atmospheric air was used, some condensation effects were present and the Reynolds number was low.

Because of the absence of any reliable methods of correcting the aerodynamic data for jet boundary effects, the data in reference 1 were presented in uncorrected form. Consequently, the comparison is made between uncorrected data from the two test facilities. Figure 3(a) presents a comparison of section normal-force coefficients and section quarter-chord moment coefficients plotted against Mach number for an NACA 64A006 airfoil section. Data from the ATA are compared with data for two test configurations of the semiopen tunnel, identified as large duct and small duct. The large (54 square inches) and small (7 square inches) ducts connected the upper and lower chambers of the test section. The small-duct data for the NACA 64A006 airfoil are from reference 1 and the large-duct data are unpublished. At low angles of attack the three sets of data are in reasonable agreement, but at high angles the agreement is not good, the normal-force coefficients having more scatter than the moment coefficients. Figure 3(b) presents the comparison of drag data from the two tunnels for the same airfoil. At zero angle of attack, the agreement

is good up to a Mach number of 0.95. At higher Mach numbers and at higher angles of attack the agreement is not as good. The differences in the data are probably attributable to a 77-percent higher Reynolds number for the present investigation and condensation effects which were present in the semiopen-tunnel tests.

In order to reduce effects of condensation in the 4- by 19-inch semiopen tunnel, a settling chamber was added and the tunnel was converted to blowdown operation from dry compressed air. The large-duct configuration was used in all tests. Figure 4 presents normal-force-coefficient and moment-coefficient data plotted against Mach number for an NACA 0012 airfoil section. The two sets of data from the two test facilities were obtained at the same stagnation pressure to eliminate effects of differences in Reynolds number. As seen from figure 4, the uncorrected data from both facilities are in close agreement when the variables of humidity and Reynolds number are eliminated.

Zero-lift drag variations with Mach number are presented in figure 5 for the NACA 65A006 and 65A009 airfoils of the present investigation and NACA 65-006 and 65-009 obtained by the falling-body method (refs. 5 and 6). The data of the present investigation are for wings of infinite aspect ratio, while the data from the falling-body tests are for a wing having an aspect ratio of 7.6. The ATA data are lower in most cases, but it must be pointed out that the ATA data are pressure-drag coefficients and have no skin friction included as do the falling-body tests. The slight difference in airfoil section is not thought to have much effect on the data. In view of the differences in aspect ratio and airfoil section, the ATA drag data show reasonable agreement with the falling-body drag data.

Corrections

The major correction to which the data of the present tests are subject is a correction to angle of attack. The theoretical value for the 1/8-open slotted ATA is about twice that given for the 4- by 19-inch semiopen tunnel (derived from ref. 7). The data of figure 4, however, indicate that the correction at low speeds for the two facilities should be about the same. Since no reliable corrections are currently available, the ATA data are presented uncorrected.

RESULTS AND DISCUSSION

Flow Photographs

Schlieren motion pictures of the flow past the models were obtained and typical frames are presented in figure 6 at angles of attack of 0°,

4°, and 8°. At Mach numbers below 1.0, the thicker section has the stronger, more fully developed shocks and a larger amount of separation than the thinner sections, as has been noted in previous investigations. (See refs. 1 and 8.) At Mach numbers above 1.0, especially after the shocks reach the trailing edge of the model, little change is noted in the flow along the model surface with increasing Mach number. The trailing-edge shocks and the bow wave, however, are subject to changes. The rearward inclination of the trailing-edge shocks increases and the bow wave approaches the leading edge with increases in Mach number. Since no abrupt changes in flow over the airfoil occur, no unusual variations of the forces are expected in this Mach number range. The Mach number for the appearance of the bow wave within the field of observation increases with increasing model thickness and angle of attack. At an angle of attack of 8° and a Mach number of 1.15 the bow wave has not entered the field (fig. 6(f)) while at 0°, (fig. 6(b)), it is visible for all thicknesses. The NACA 64A006 schlieren model was about 0.01 inch short of spanning the tunnel. At angles of attack of 4° and 8°, the model-wall clearance allowed some flow to pass along the side of the model and into the tunnel-wall boundary layer, causing the flow pattern noted in figures 6(c) to 6(f) along the upper surface of the model.

Experience in transonic research indicated that the model bow wave might be reflected back onto the model and cause discontinuities in the pressure distributions along the model surface and produce errors in the measurement of the aerodynamic forces. In a few frames from all the pictures of the present investigation a very weak reflection was observed to cross the model wake well behind the model. As the Mach number was decreased this reflection moved forward but faded out before it reached the model. An examination of pressure distributions and manometer-board records confirmed the absence of reflections for these tests.

Aerodynamic Forces

The basic force characteristics of each of the four airfoils tested are presented in figure 7 as a function of Mach number and angle of attack. These forces are discussed separately in the following sections.

Lift.- Section lift coefficients for the airfoils are presented in figure 8 as a function of angle of attack. For easier analysis these data have been replotted in figure 9(a) as lift-curve slope against Mach number for various lift coefficients. At high subsonic speeds and for all supersonic speeds the thinnest airfoils have the highest lift-curve slope. As the Mach number increases above 1.0, however, the curves for the different thicknesses converge and seem to be approaching a limiting value.

Lift-curve slope plotted against Mach number for a lift coefficient of 0.2 is compared in figure 9(b) with slopes calculated by the second-order supersonic theory of reference 9. The theory, applicable only for

sharp-nosed airfoils above the Mach number for shock attachment was developed for thin airfoils at low angles of attack. The data for all thicknesses seem to be converging and approaching the theoretically predicted supersonic values as an upper limit. Schlieren photographs show no changes in the flow along the surface after the shocks have reached the trailing edge. An examination of the pressure distributions over the model showed supersonic velocities to be existing over nearly the entire airfoil surface, except for a small percent of the chord near the leading edge. Thus, it is expected that the experimental data should agree reasonably well with supersonic theory, although the bow wave is detached. (See also refs. 10 and 8.)

Drag.- Section drag coefficients plotted against section lift coefficient at various Mach numbers for the airfoils tested are presented in figures 10(a) and 10(b). Values of pressure drag at zero and 0.4 lift coefficients are presented in figures 10(c) and 10(d), respectively, and are compared with second-order supersonic theory for circular-arc airfoil sections. The ticks on the theoretical curves indicate the Mach number for flow attachment, based on a deflection angle of one-half the leading-edge angle plus the angle of attack. The experimental data in figure 10(c) reach a peak value at a Mach number of about 1.0 and decrease slightly as the Mach number is increased above 1.0.

At the maximum test Mach number, 1.25, the drag coefficients for the thinnest airfoils are above the theoretical values for circular-arc sections. It must be remembered that the theory is only applicable above the shock attachment Mach number noted on the curves, but it has been extended to lower speeds for comparison purposes. Higher drag coefficients are to be expected on the blunt-nose 6A-series airfoils than on the sharp-nose airfoils of the theory, due to the higher pressures on the blunt nose. Drag data on an NACA 65-009 airfoil from reference 10 at a Mach number of 1.62 are also presented in figures 10(c) and 10(d) and are higher than the theoretical values. Also shown in figure 10(c) are data for a circular-arc airfoil at a Mach number of 1.62 (from ref. 10 (derived from ref. 11)). These experimental circular-arc data fall slightly below the theoretical value, due to flow separation at the trailing edge. The data in figure 10(d) at a lift coefficient of 0.4 indicate the same trends as observed in figure 10(c) at zero lift, except that drag coefficients tend to increase with increasing Mach number. The agreement between experimental and theoretical drag coefficients is not as good as that noted in the other forces.

Lift-drag ratios are presented in figure 11(a) as a function of lift coefficient for several Mach numbers. For Mach numbers below 1.0, the general variation is quite similar to previously published results, the lift-drag ratios decreasing as lift coefficient is increased beyond about 0.3. At supersonic Mach numbers, however, the lift-drag ratios remain about constant in the high lift-coefficient range. At all lift

coefficients for Mach numbers of 0.90 and above, the thinnest profile has the highest lift-drag ratios, and the effects of changes in shape between the NACA 65A006 and NACA 64A006 airfoil sections are insignificant.

Maximum lift-drag ratios as a function of Mach number for the 65A-series airfoils are compared in figure 11(b) with second-order supersonic theory for circular-arc airfoil sections. The experimental data show very good agreement with the extension of the theoretical values.

Moment.- Section quarter-chord moment coefficients are presented in figure 12 as a function of section lift coefficient for several Mach numbers. At Mach numbers from 0.925 to 0.975, the thick airfoil (NACA 65A009) has a rapid increase followed by a rapid decrease in moment coefficient as lift coefficient is increased. The difference is due to the large amount of separation on the upper surface and rearward location of the lower surface shock as seen in figure 6(c) and also is noted in the basic data of figure 7(d). The thinner sections, however, have a continual decrease in moment coefficient throughout the range of lift coefficients investigated. At supersonic Mach numbers, the decrease in moment coefficient with increase in lift is nearly linear for all thicknesses and the slopes of the moment curves remain about the same for all supersonic Mach numbers.

Figure 13(a) presents the chordwise variations in location of center of pressure with Mach number at lift coefficients of 0.1, 0.2, and 0.4 for the three 65A-series airfoils. For Mach numbers from 0.8 to about 0.95 the center of pressure moves rearward on the thin airfoils, reaching about the 0.45 chord position at the low lift coefficient. The thick airfoil, however, has a large forward movement of center of pressure, which is maximum at a Mach number of about 0.95. For Mach numbers above about 1.05, the center of pressure remains around the 0.41 chord station for all the airfoils.

The location of center of pressure at the highest Mach number obtained in the tests is in good agreement with second-order supersonic theory for circular-arc airfoil sections as seen in figure 13(b).

Correlation on Basis of Transonic Similarity Laws

Zero-lift drag, lift-drag ratio, and lift-curve-slope data for the 65A-series airfoils are compared by transonic similarity laws in figure 14. The similarity parameter used is that presented in references 12 and 13. The comparison of zero-lift drag is presented in figures 14(a) and 14(b). In figure 14(a) the reduced drag coefficient is plotted against reduced Mach number and the correlation is reasonably good at Mach numbers below 1.0 ($\xi < 0$). At sonic and supersonic speeds ($\xi \geqq 0$) the correlation is poor. In figure 14(b) the thickness term in the reduced drag coefficient

has been reduced from the theoretical 5/3 power (1.67) to the 3/2 power (1.50) and the correlation is greatly improved. This reduction in the exponent of the thickness term was also noted in reference 14 to be necessary at $M = 1.0$ to provide correlation of pressure coefficient at the maximum thickness location.

Lift-curve slopes at zero lift are presented in figure 14(c). The correlation of the effects of thickness is good at supersonic Mach numbers. Although there is fair agreement between the data for the 4- and 6-percent-thick airfoils, the coefficients for the 9-percent-thick airfoil diverges considerably. This difference is due to the large amount of separation on the upper surface and more rearward position of the lower surface shock on the 9-percent-thick airfoil which is not encountered on the thinner airfoils (fig. 6).

Figure 14(d) presents the correlation of maximum lift-drag ratios for the three airfoils. Although there is some scatter in the results, the correlation is considered to be very good. No alteration has been made to the theoretical exponent of the thickness term in lift-drag ratio and lift-curve slope as was made in the correlation of drag coefficient.

CONCLUSIONS

A two-dimensional wind-tunnel investigation of the flow and force characteristics of four NACA 6A-series airfoils with thickness ratios of 4, 6, and 9 percent has been conducted in the Langley airfoil test apparatus at transonic Mach numbers between 0.8 and 1.25. An analysis of the data from this investigation has led to the following conclusions:

1. At subsonic speeds, flow and force characteristics were in agreement with results from previous investigations. The airfoil sections exhibited a smooth transition from Mach number 1.0 to the values obtained at the higher speeds.

2. Lift-curve slopes, lift-drag ratios, and center-of-pressure locations at the supersonic speeds were in reasonably good agreement with second-order supersonic theory for doubly symmetrical circular-arc sections of the same thickness ratio. Drag coefficients were higher than the theoretical value for sharp-nosed airfoils which is a natural result of flows with detached shocks.

3. Lift-curve slope and maximum lift-drag ratio correlated very well at supersonic speeds by the transonic similarity laws. At Mach numbers below 1.0, the correlation was not good. Correlation of drag coefficient, however, was not good at supersonic speeds unless the

exponent of the thickness term was reduced from the theoretical value of 1.67 to 1.50, thus reducing the effects of the thickness.

Langley Aeronautical Laboratory,
National Advisory Committee for Aeronautics,
Langley Field, Va., May 17, 1957.

REFERENCES

1. Daley, Bernard N., and Dick, Richard S.: Effect of Thickness, Camber, and Thickness Distribution of Airfoil Characteristics at Mach Numbers Up to 1.0. NACA TN 3607, 1956. (Supersedes NACA RM L52G31a.)

2. Amick, J. L., Clark, E. T., Culbertson, P. E., McLeish, W. M., and Liepman, H. P.: Wind Tunnel Tests of Seventeen Airfoils at Supersonic Speeds. Rep. No. WTM-240 (Contract AF-33(038)-17737 - Part I E. O. No. 587-145 BR-1), Eng. Res. Inst., Univ. Mich., Mar. 1953.

3. Fitzpatrick, J. E., and Rice, Janet B.: Aerodynamic Characteristics of Seventeen Airfoil Sections at Transonic Mach Numbers. Rep. R-25473-22 (Contract AF 33(038)-2209), United Aircraft Corp. Res. Dept., Apr. 30, 1953.

4. Humphreys, Milton D.: Pressure Pulsations on Rigid Airfoils at Transonic Speeds. NACA RM L51I12, 1951.

5. Thompson, Jim Rogers, and Marschner, Bernard W.: Comparative Drag Measurements at Transonic Speeds of an NACA 65-006 Airfoil and a Symmetrical Circular-Arc Airfoil. NACA RM L6J30, 1947.

6. Mathews, Charles W., and Thompson, Jim Rogers: Drag Measurements at Transonic Speeds of NACA 65-009 Airfoils Mounted on a Freely Falling Body To Determine the Effects of Sweepback and Aspect Ratio. NACA RM L6K08c, 1947.

7. Katzoff, S., Gardner, Clifford S., Diesendruck, Leo, and Eisenstadt, Bertram J.: Linear Theory of Boundary Effects in Open Wind Tunnels With Finite Jet Lengths. NACA Rep. 976, 1950. (Supersedes NACA TN 1826.)

8. Lindsey, Walter F., and Dick, Richard S.: Two-Dimensional Chordwise Load Distributions at Transonic Speeds. NACA RM L51I07, 1952.

9. Lock, C. N. H.: Examples of the Application of Busemann's Formula To Evaluate the Aerodynamic Force Coefficients on Supersonic Aerofoils. R. & M. No. 2101, British A.R.C., 1944.

10. Rainey, Robert W.: Pressure Measurements at Supersonic Speeds on a Section of a Rectangular Wing Having an NACA 65-009 Profile. NACA RM L9L16, 1950.

11. Czarnecki, K. R., and Mueller, James N.: Investigation at Mach Number 1.62 of the Pressure Distribution Over a Rectangular Wing With Symmetrical Circular-Arc Section and 30-Percent-Chord Trailing-Edge Flap. NACA RM L9J05, 1950.

12. Busemann, Adolf: Application of Transonic Similarity. NACA TN 2678, 1952.

13. Spreiter, John R.: On the Application of Transonic Similarity Rules to Wings of Finite Span. NACA Rep. 1153, 1953. (Supersedes NACA TN 2726.)

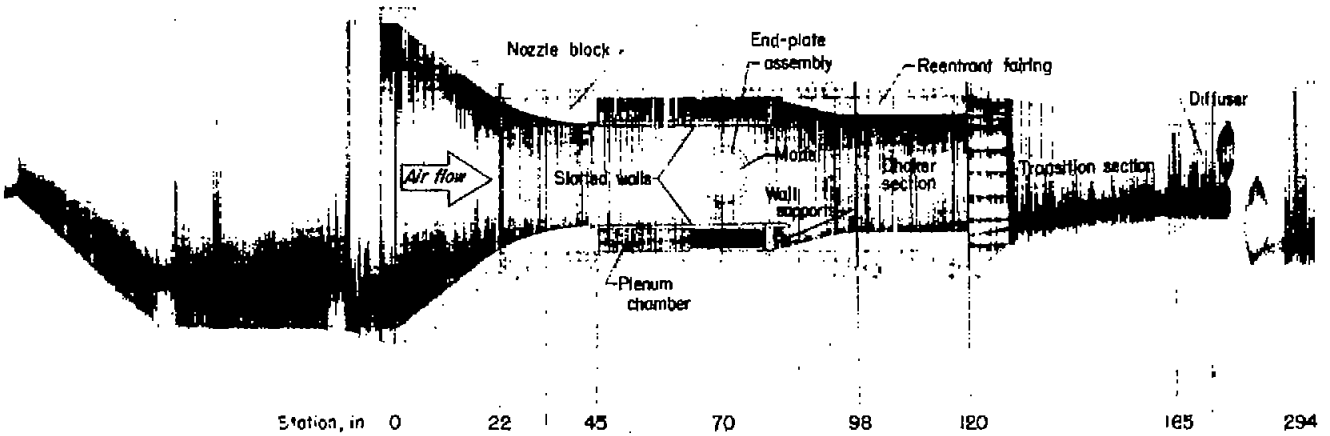

(a) General view. L-57-599

Figure 1.- Langley airfoil test apparatus.

CONFIDENTIAL

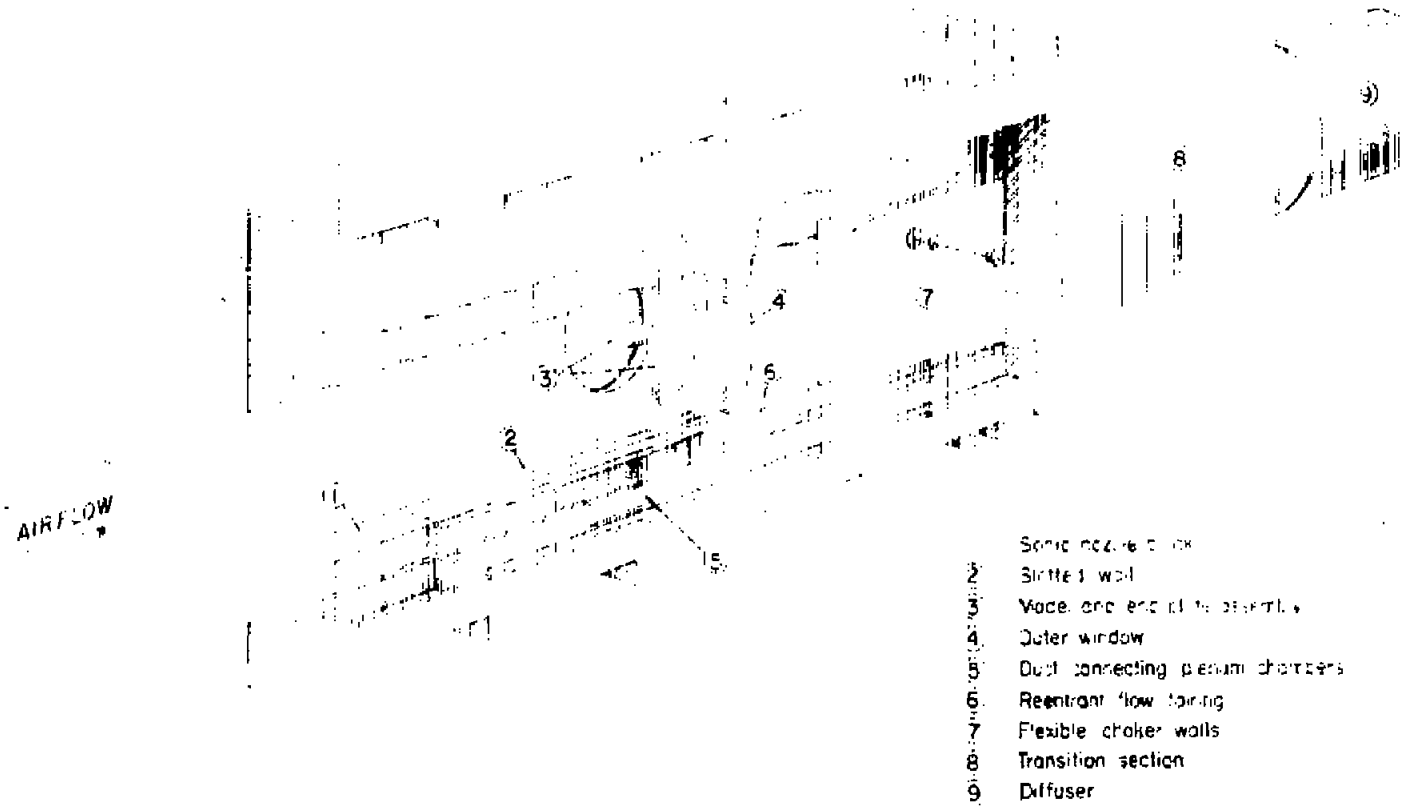

(b) Test section. L-57-598

Figure 1.- Concluded.

CONFIDENTIAL

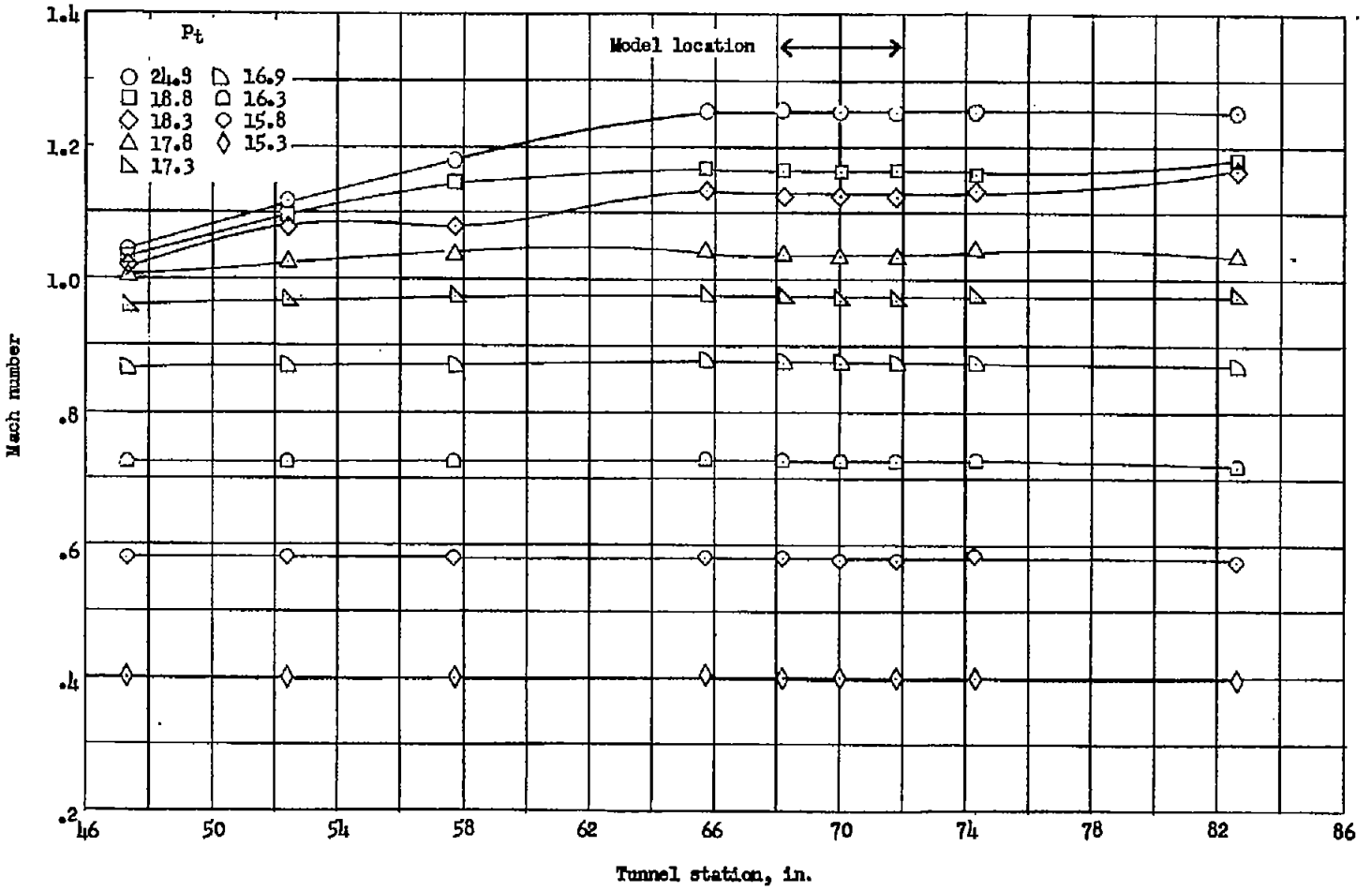

Figure 2.- Mach number distribution through test section.

UNCLASSIFIED

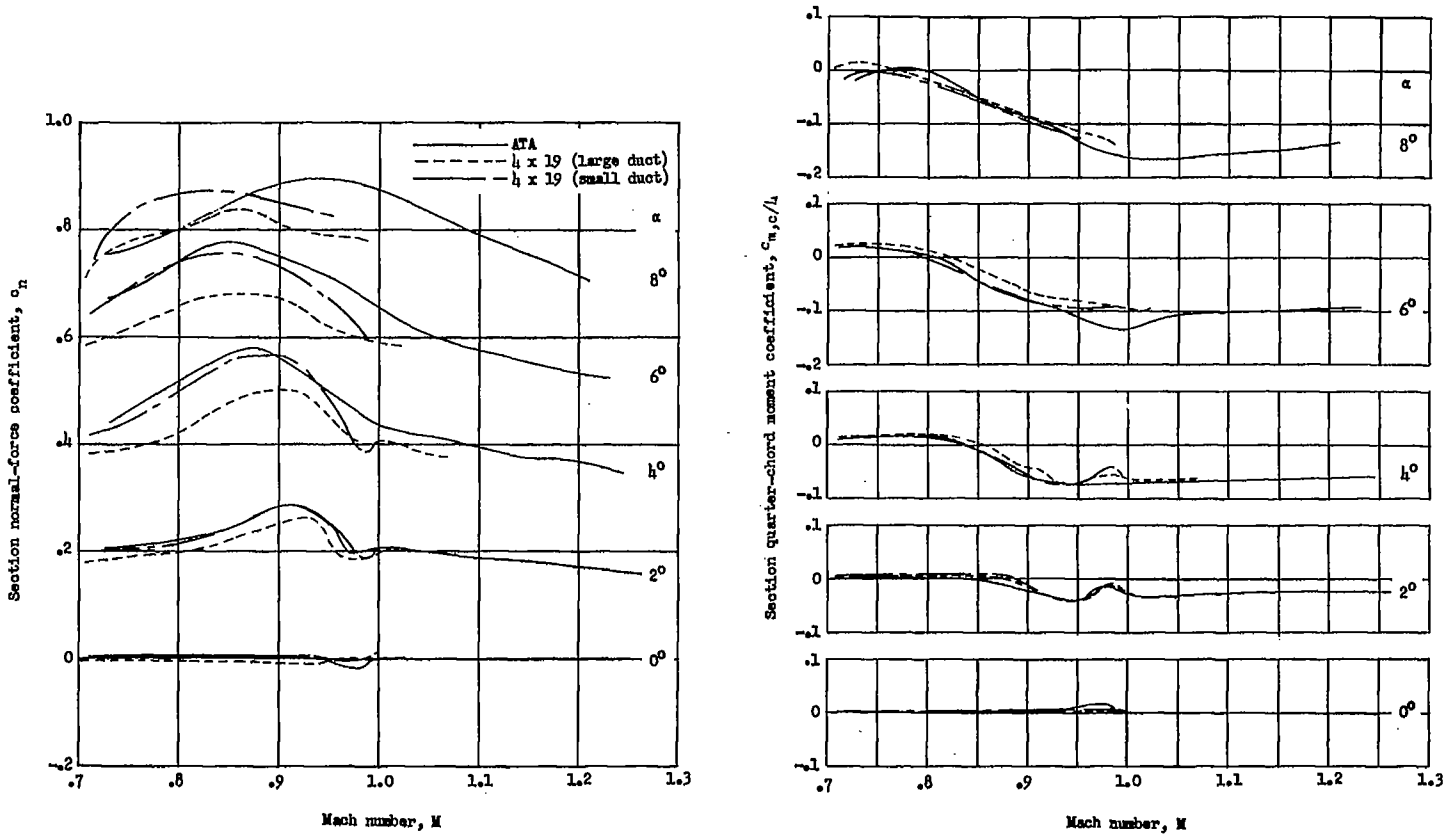

(a) Normal-force and moment coefficient.

Figure 3.- Comparison of data obtained on an NACA 64A006 airfoil in Langley airfoil test apparatus (ATA) with data from Langley 4- by 19-inch semiopen tunnel.

UNCLASSIFIED

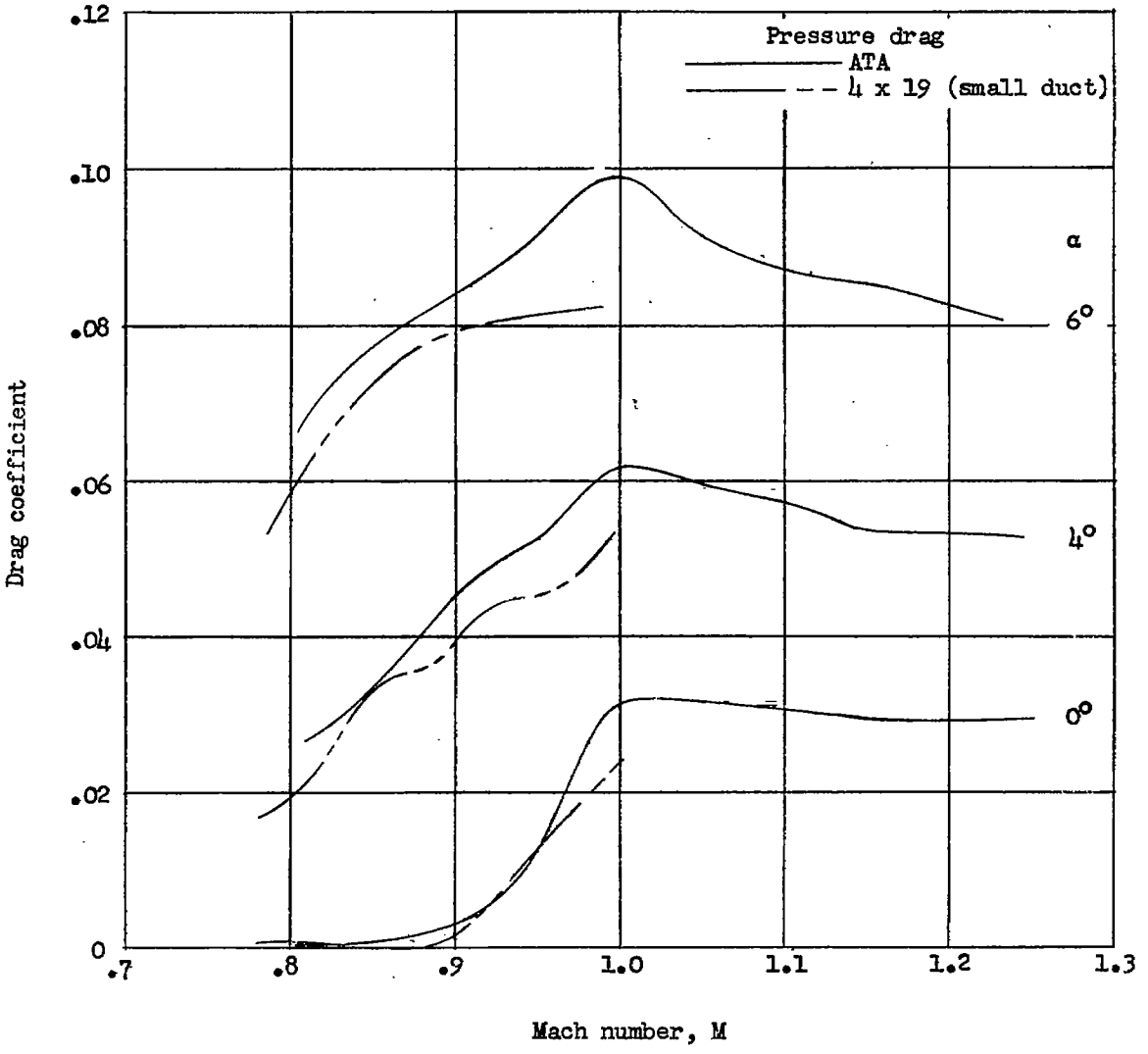

(b) Drag coefficient.

Figure 3.- Concluded.

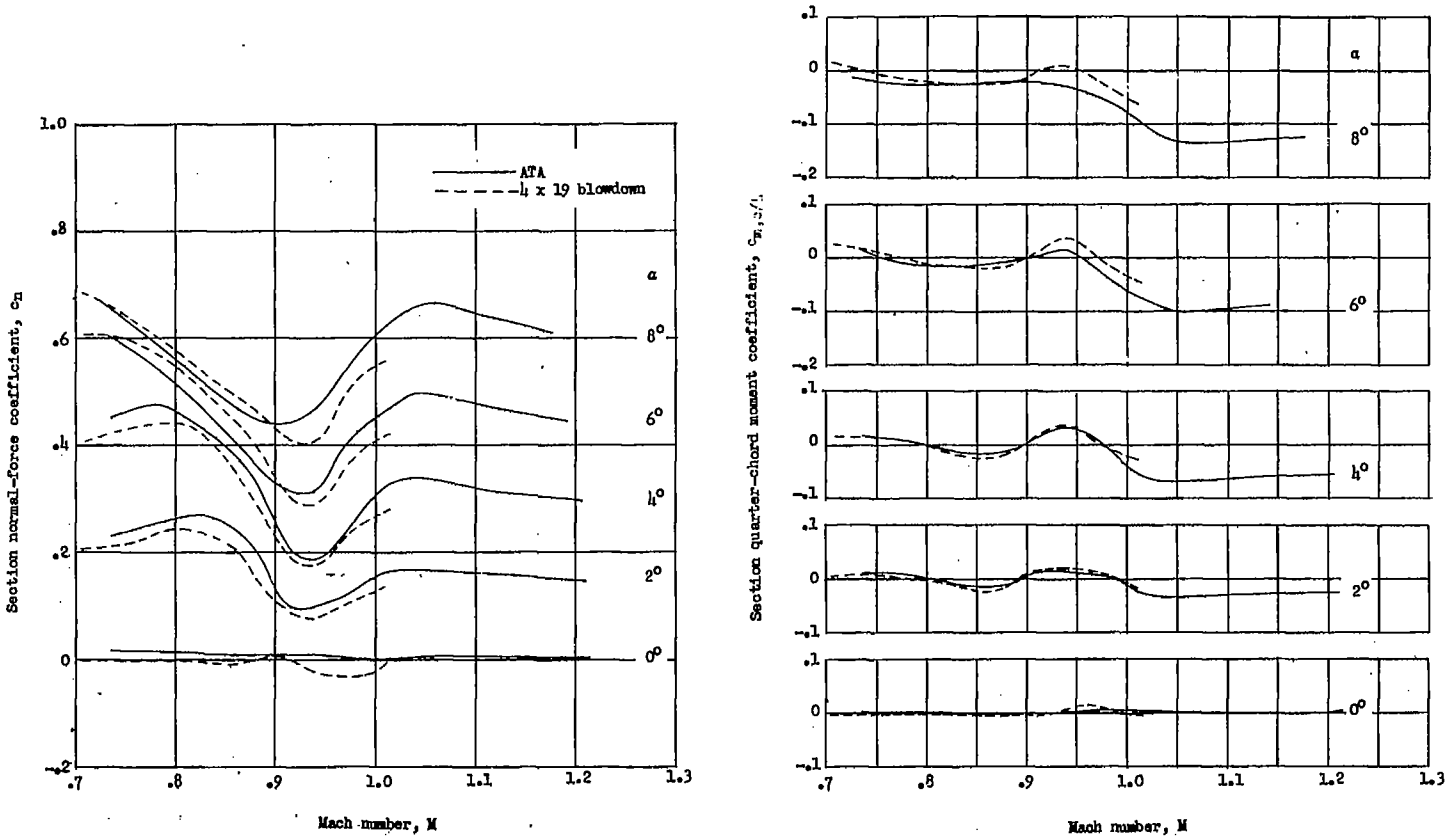

Figure 4.- Comparison of data obtained on an NACA 0012 airfoil in Langley airfoil test apparatus (ATA) with data from 4- by 19-inch semiopen tunnel converted to blowdown operation.

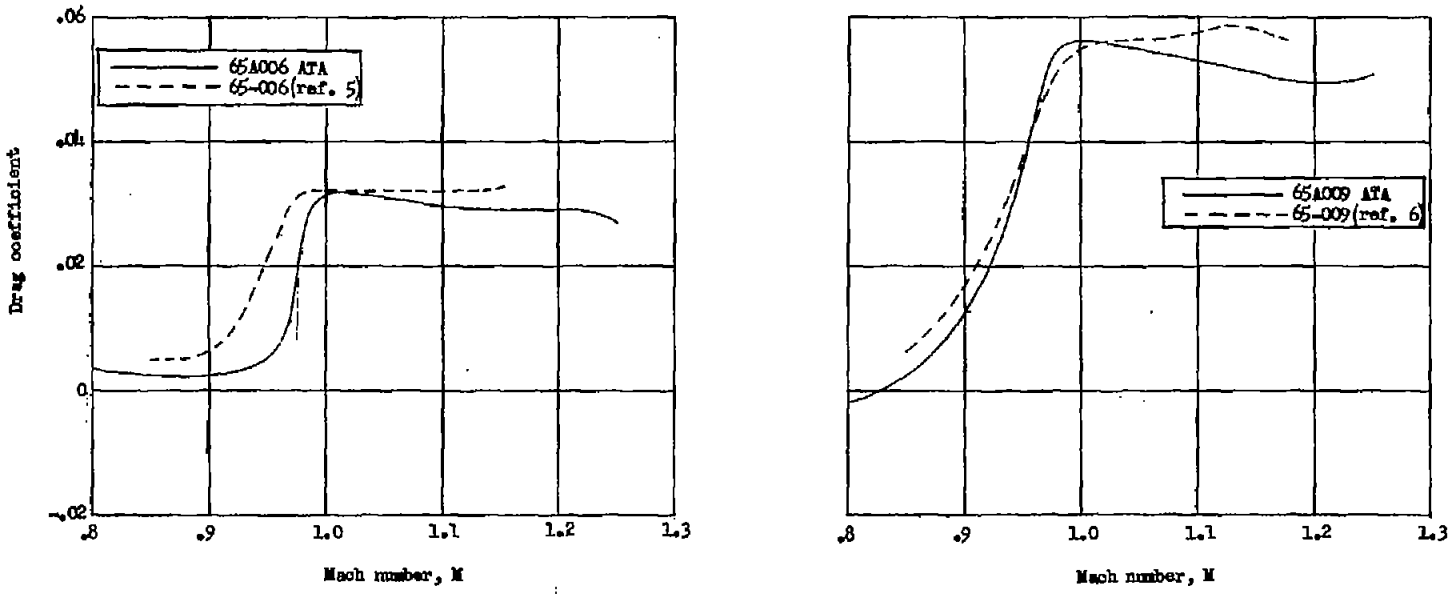

Figure 5.- Comparison of zero-lift drag coefficients obtained in Langley airfoil test apparatus (ATA) with those obtained from free-fall tests.

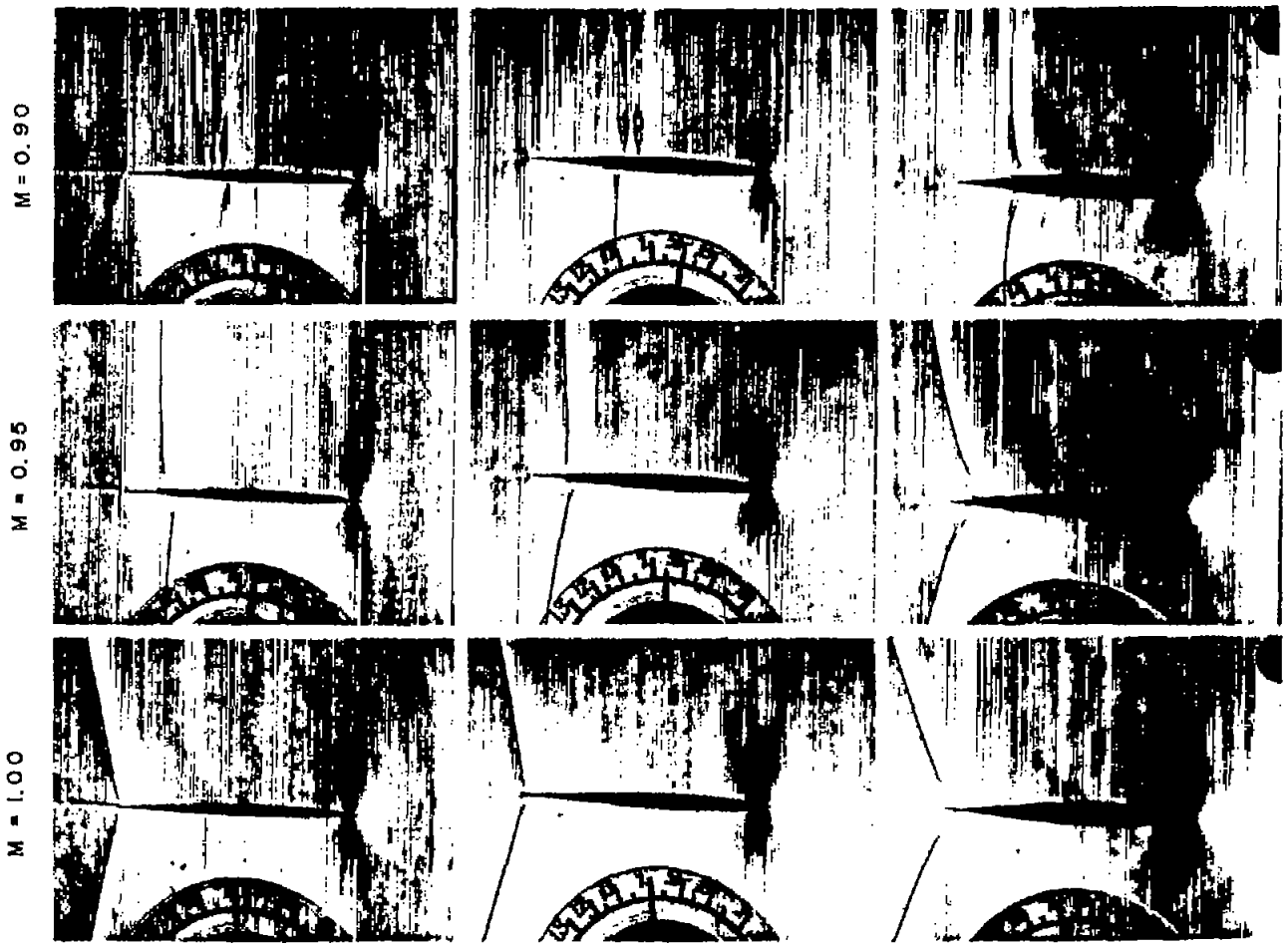

(a) $\alpha = 0^{\circ}$.

L-57-1598

Figure 6.- Schlieren flow photographs.

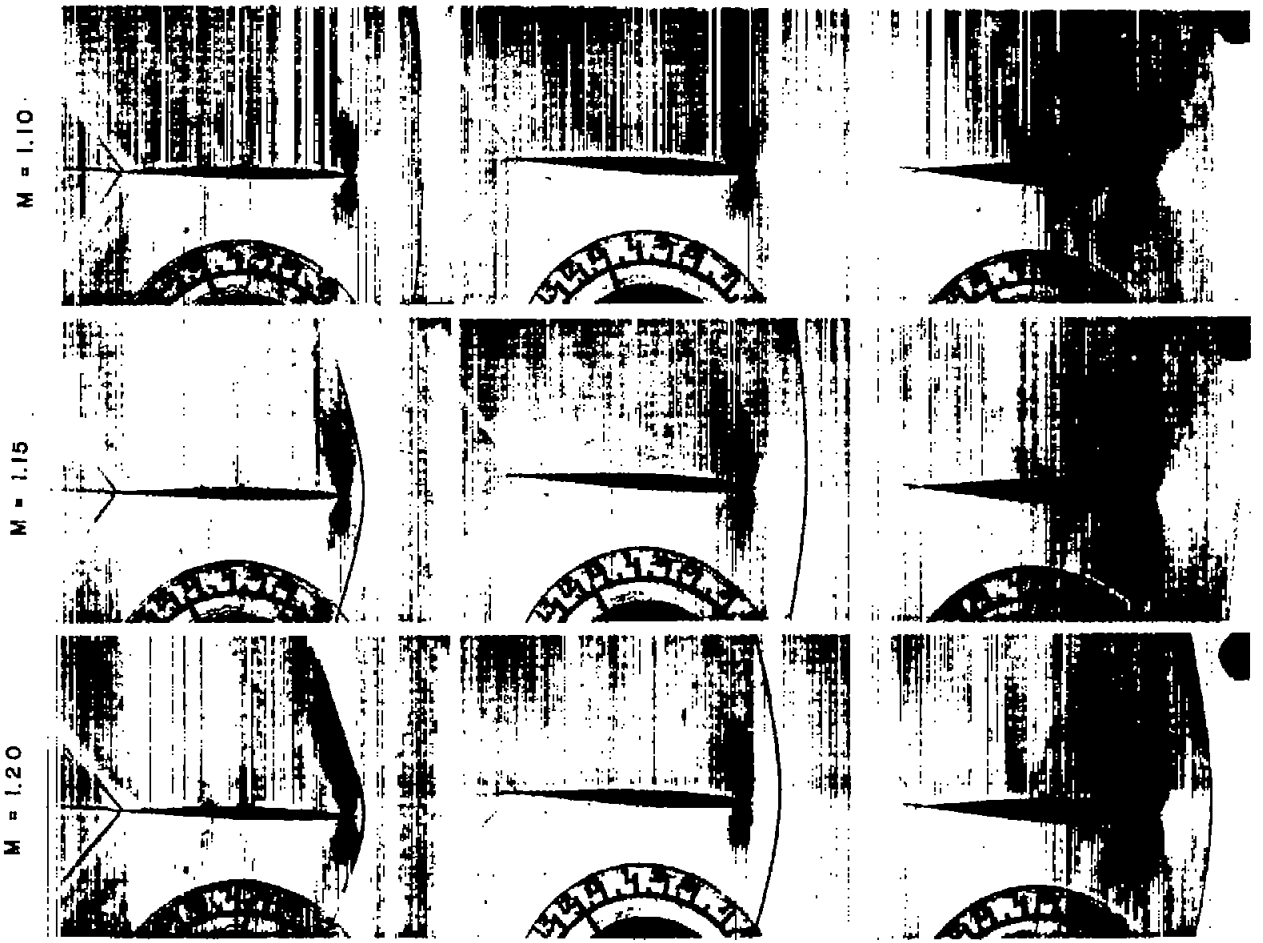

(b) $\alpha = 0^{\circ}$.

L-57-1599

Figure 6.- Continued.

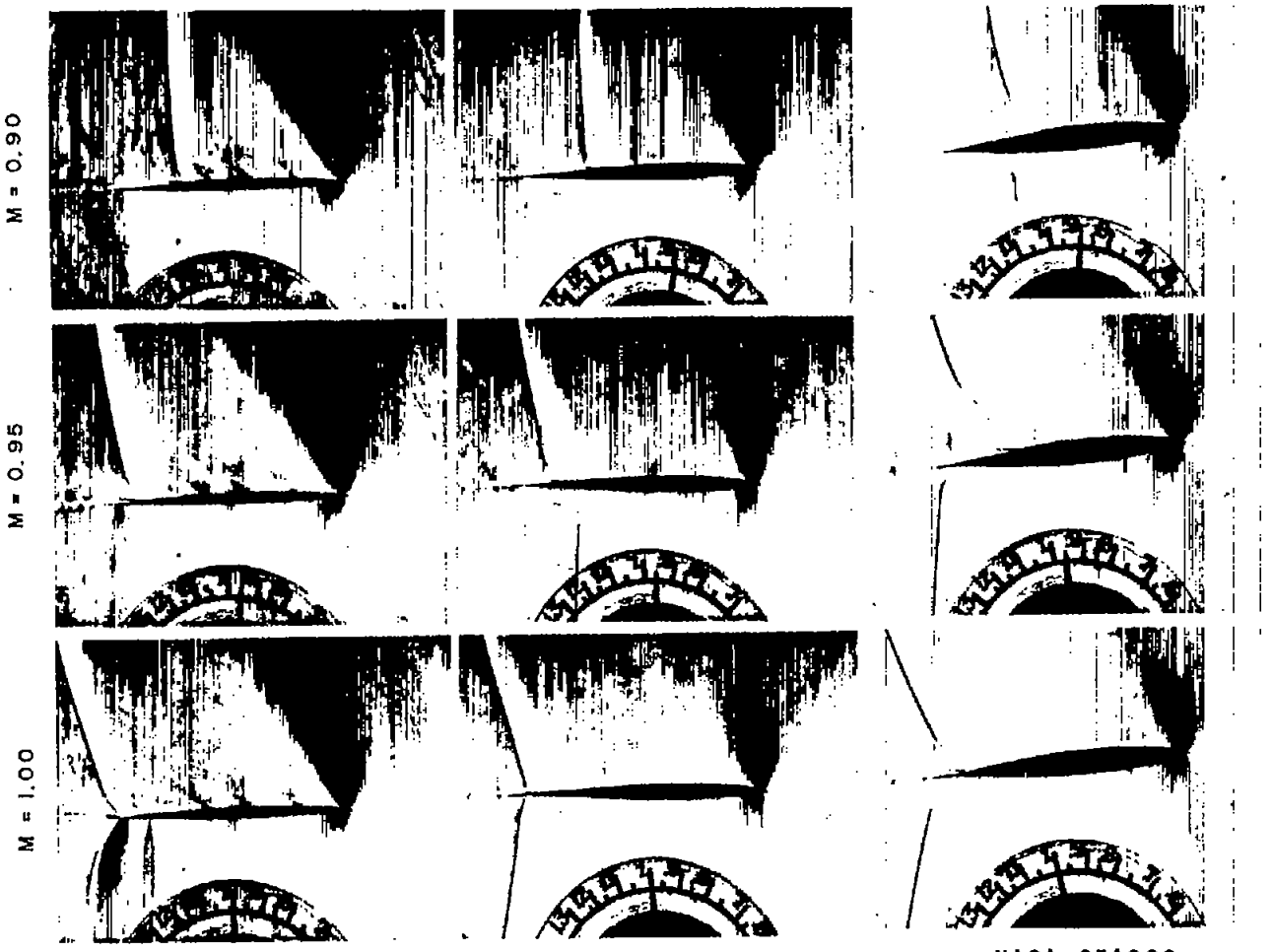

NACA 65A004 NACA 65A006 NACA 65A009

(c) $\alpha = 4^{\circ}$.

L-57-1600

Figure 6.- Continued.

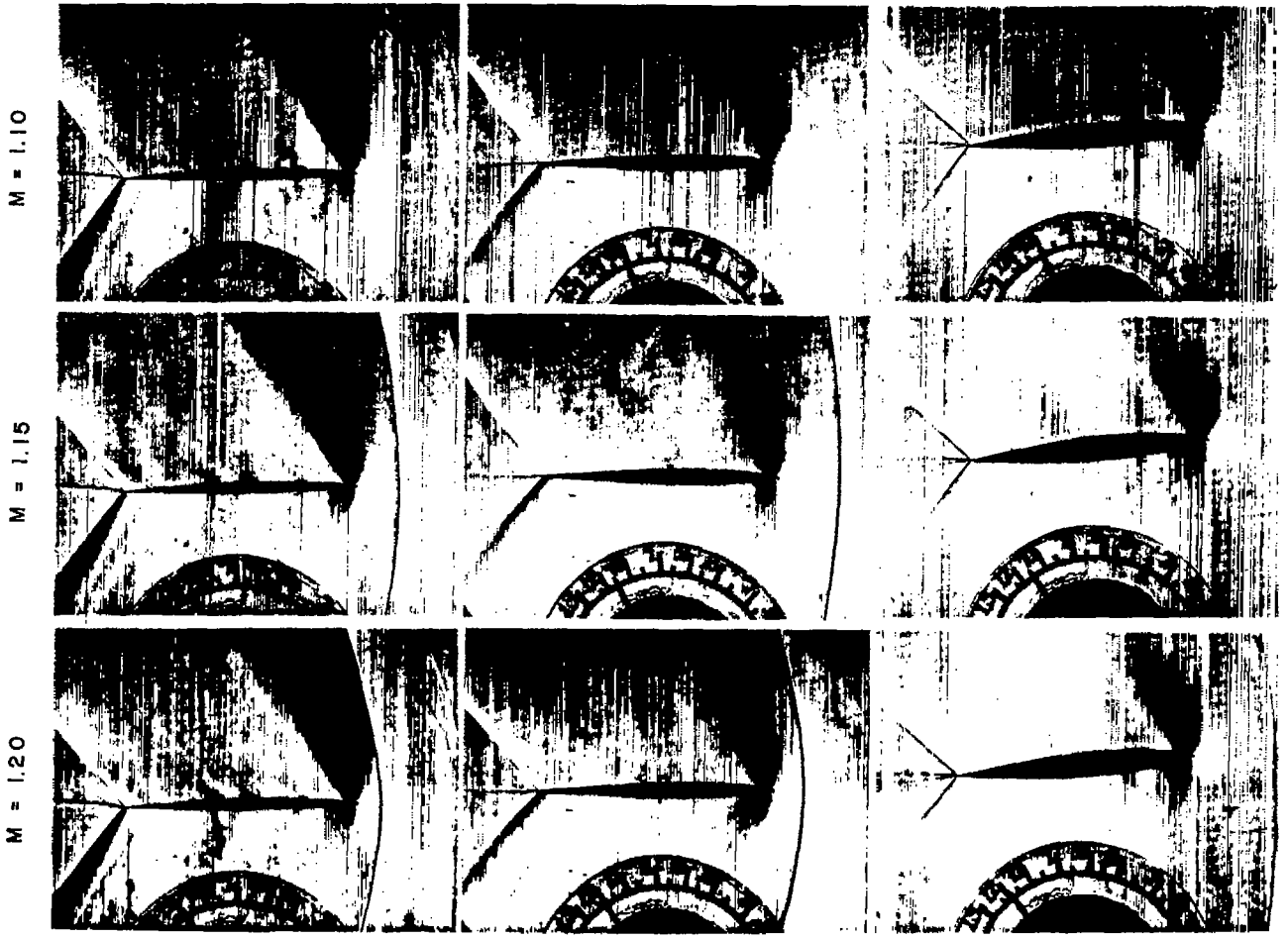

(d) $\alpha = 4^{\circ}$.

L-57-1601

Figure 6.- Continued.

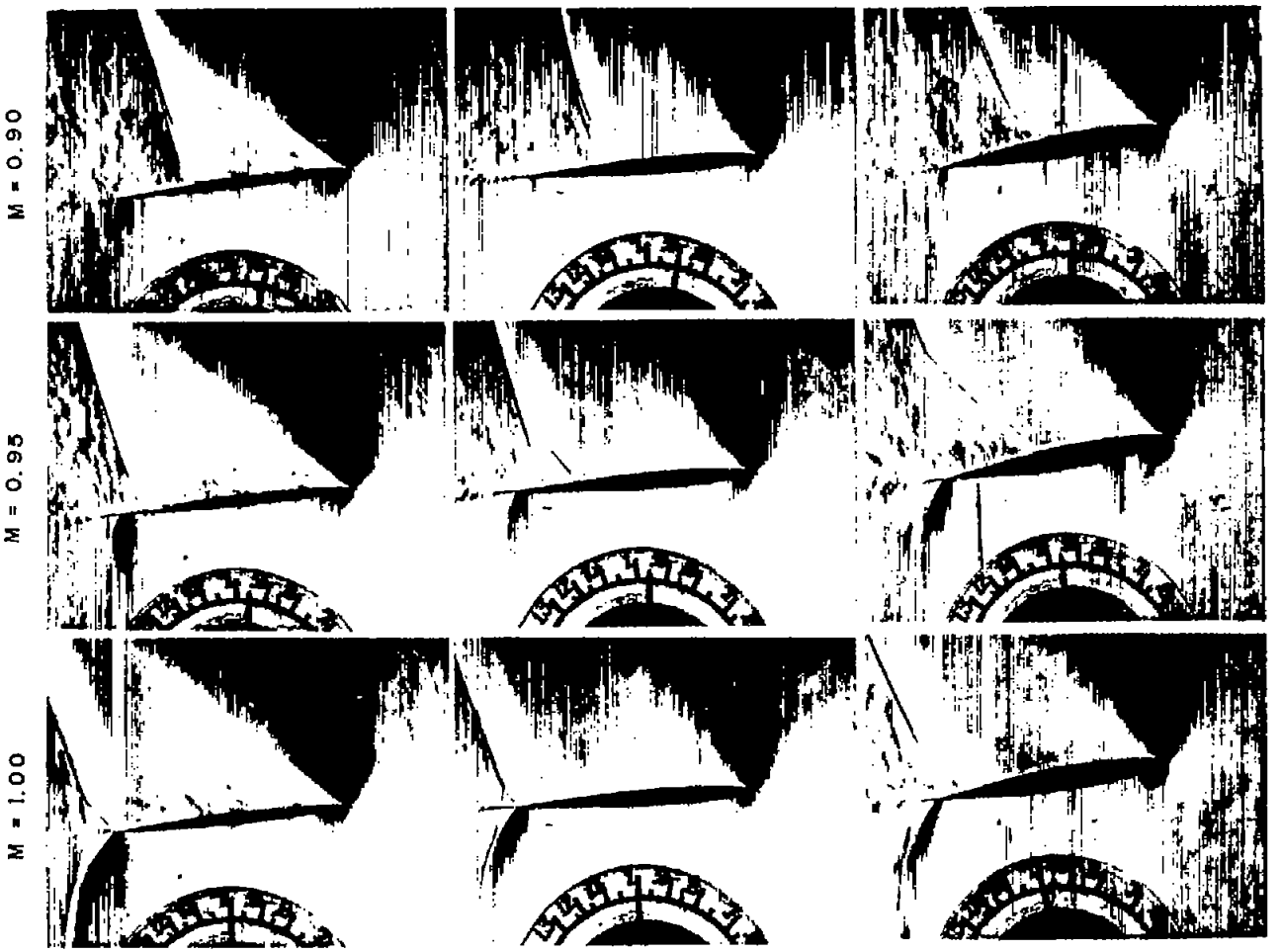

NACA 65A004 NACA 65A006 NACA 65A009

(e) $\alpha = 8^{\circ}$. L-57-1602

Figure 6.- Continued.

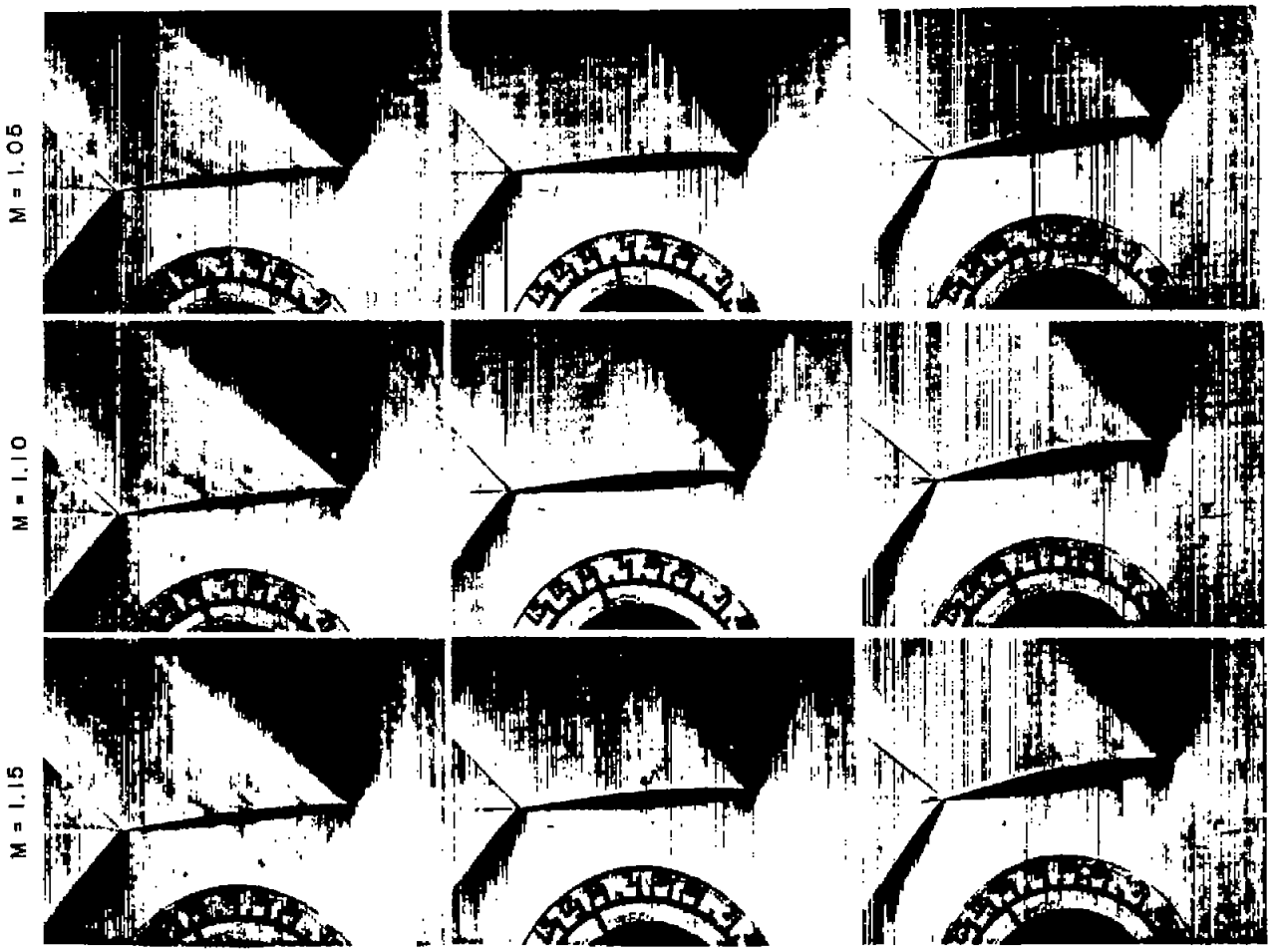

(f) $\alpha = 8^{\circ}$.

L-57-1603

Figure 6.- Concluded.

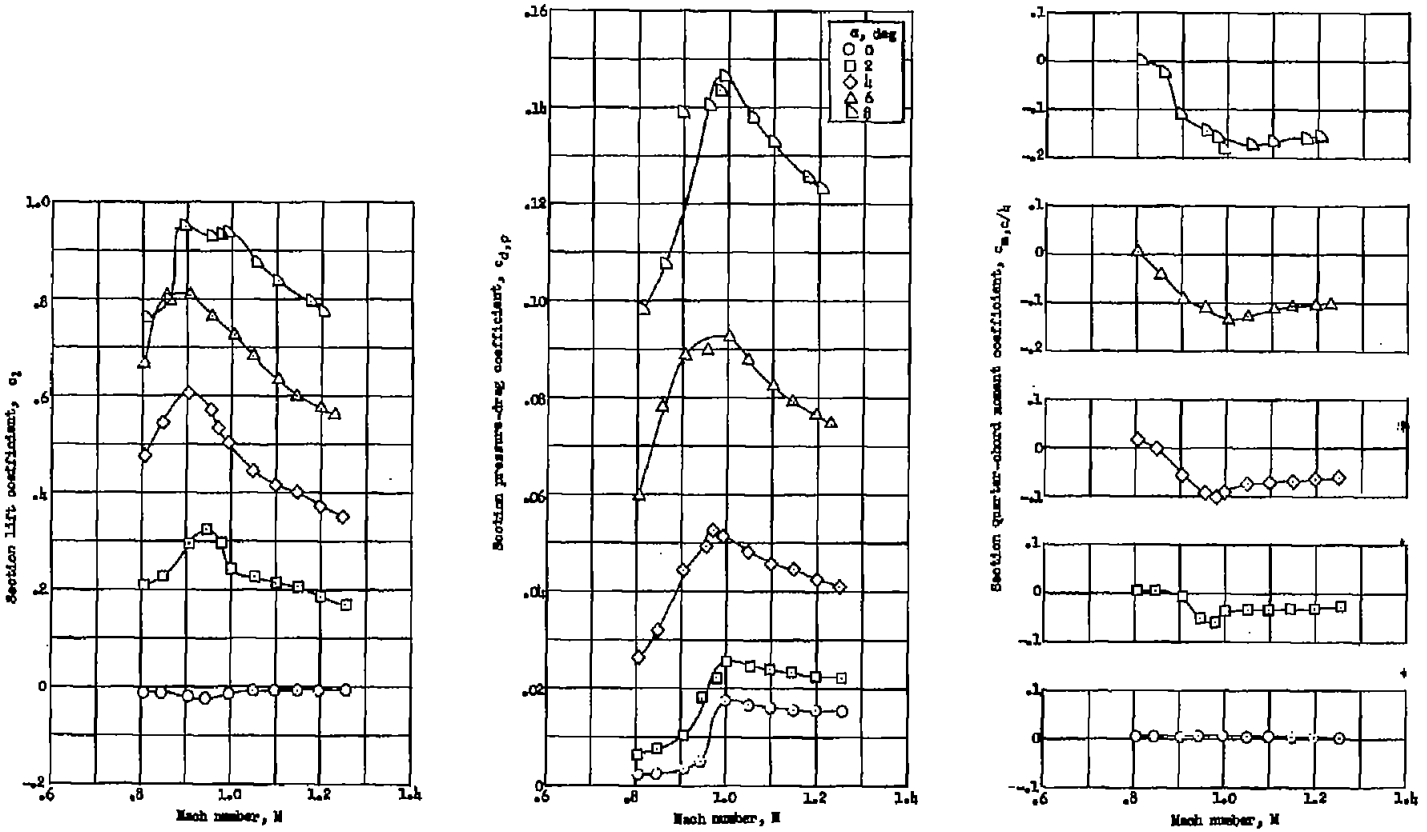

(a) NACA 65A004 airfoil section.

Figure 7.- Variations of airfoil-section characteristics with Mach number.

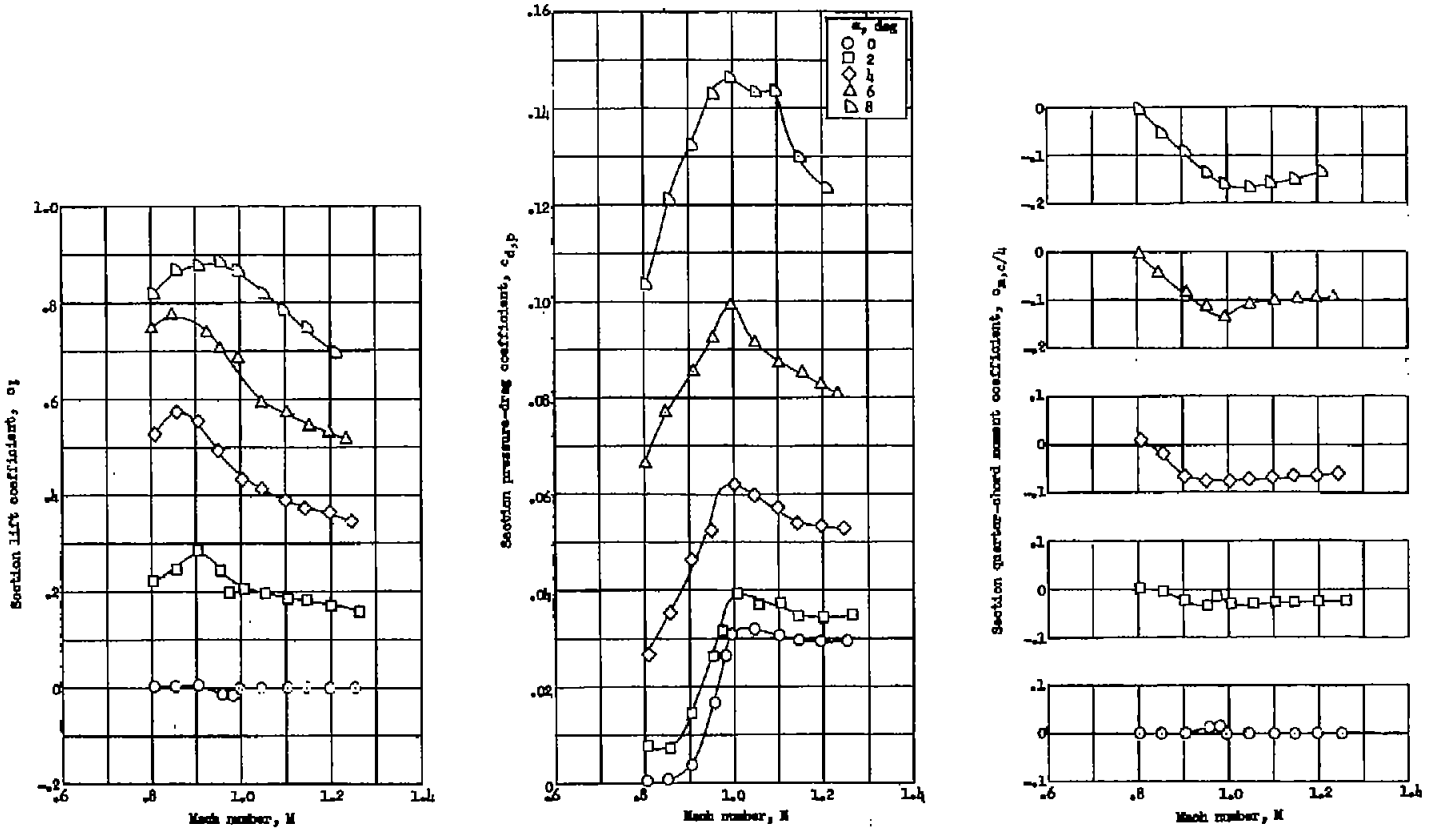

(b) NACA 64A006 airfoil section.

Figure 7.- Continued.

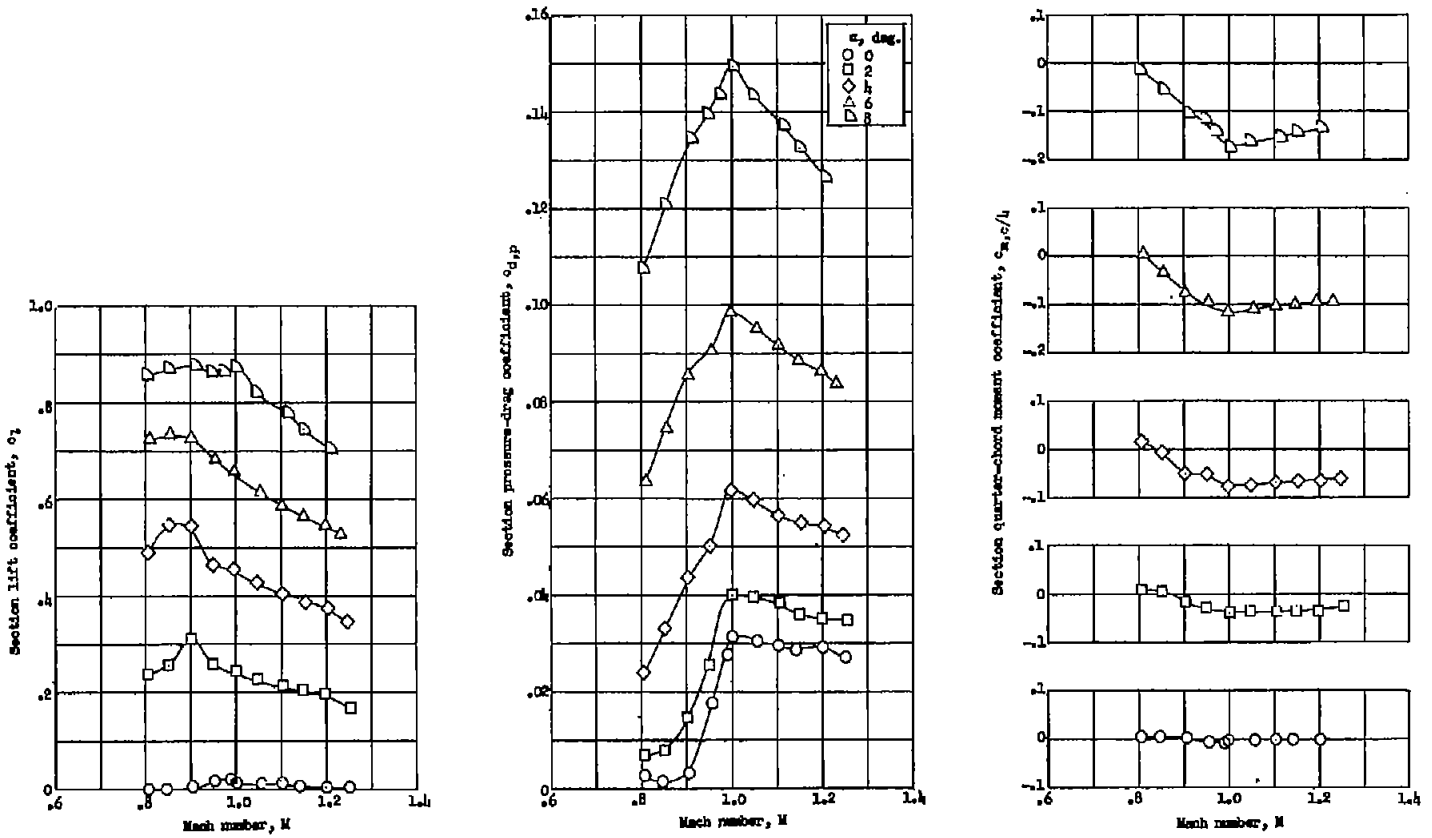

(c) NACA 65A006 airfoil section.

Figure 7.- Continued.

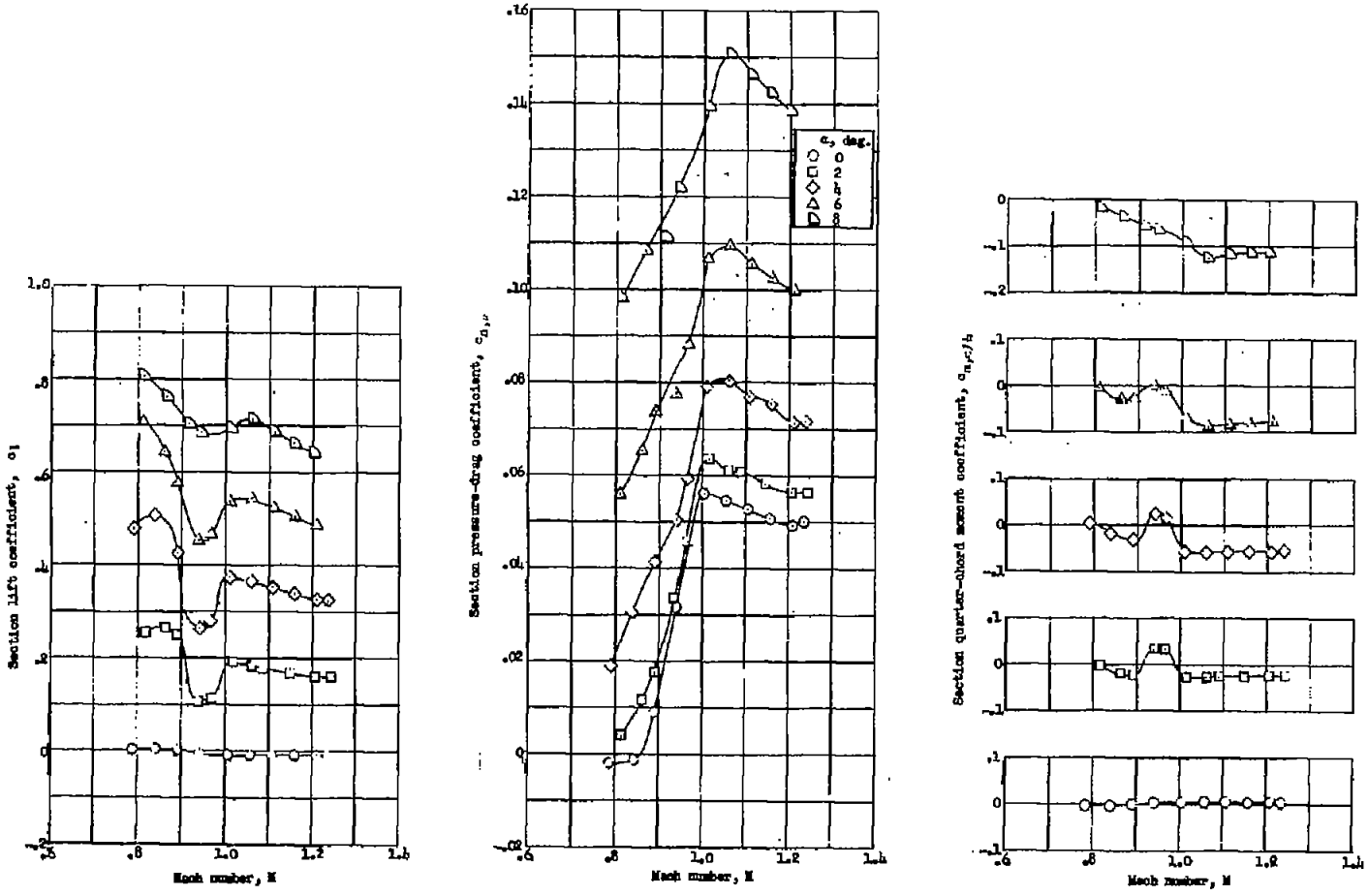

(d) NACA 65A009 airfoil section.

Figure 7.- Concluded.

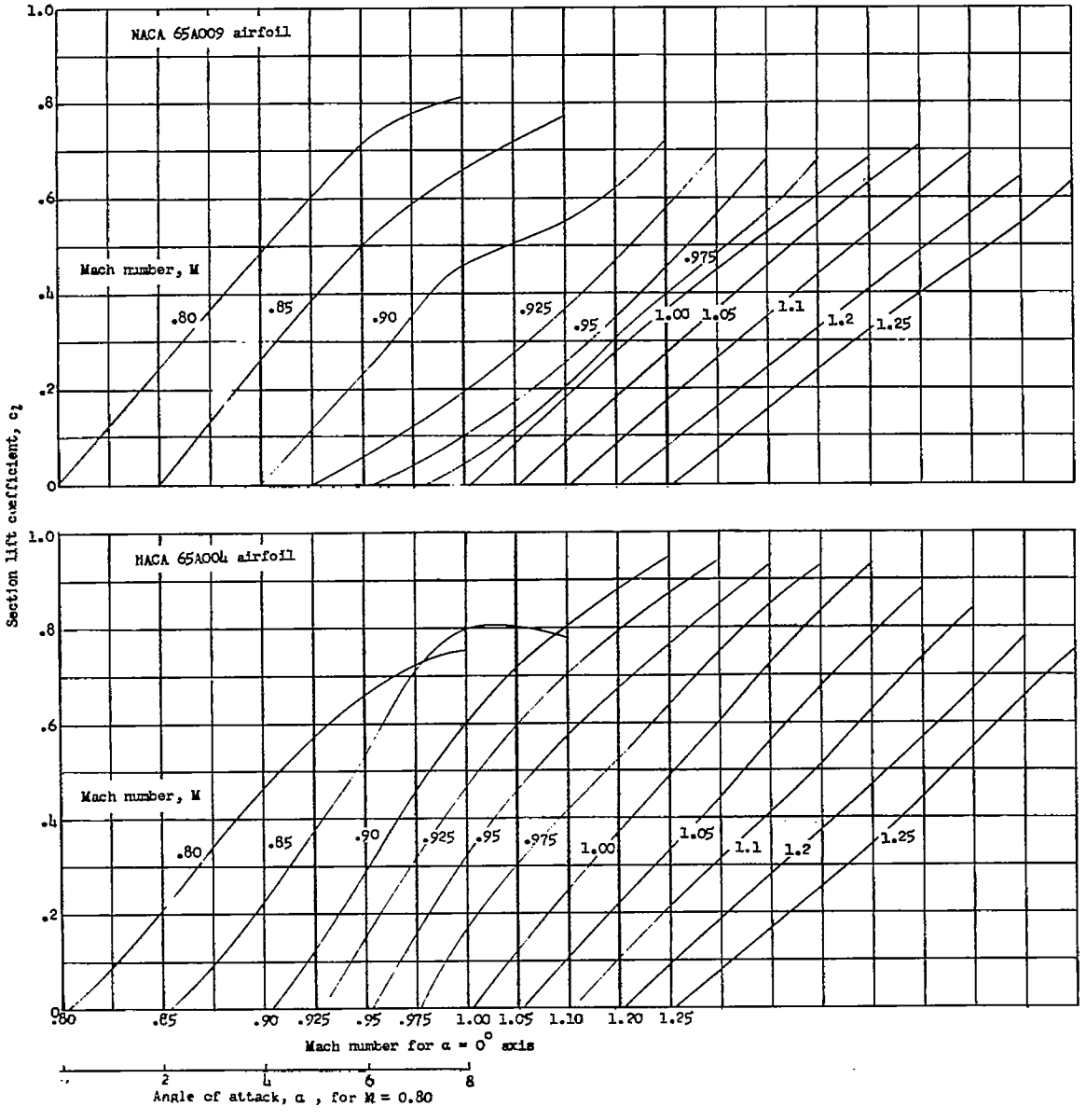

(a) NACA 65A004 and NACA 65A009 sections.

Figure 8.- Variations in section lift coefficient with angle of attack for various Mach numbers.

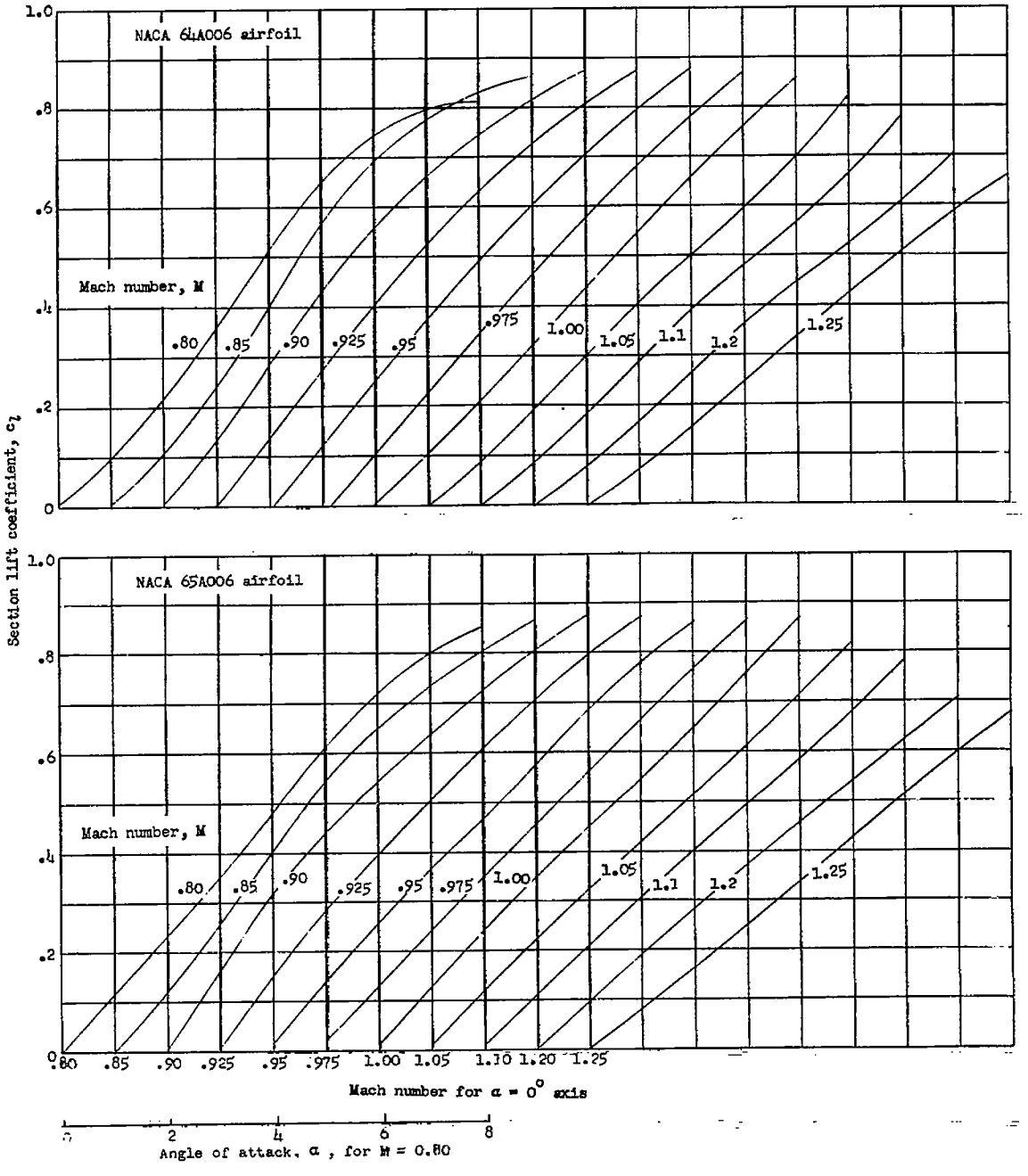

(b) NACA 65A006 and NACA 64A006 sections.

Figure 8.- Concluded.

CONFIDENTIAL

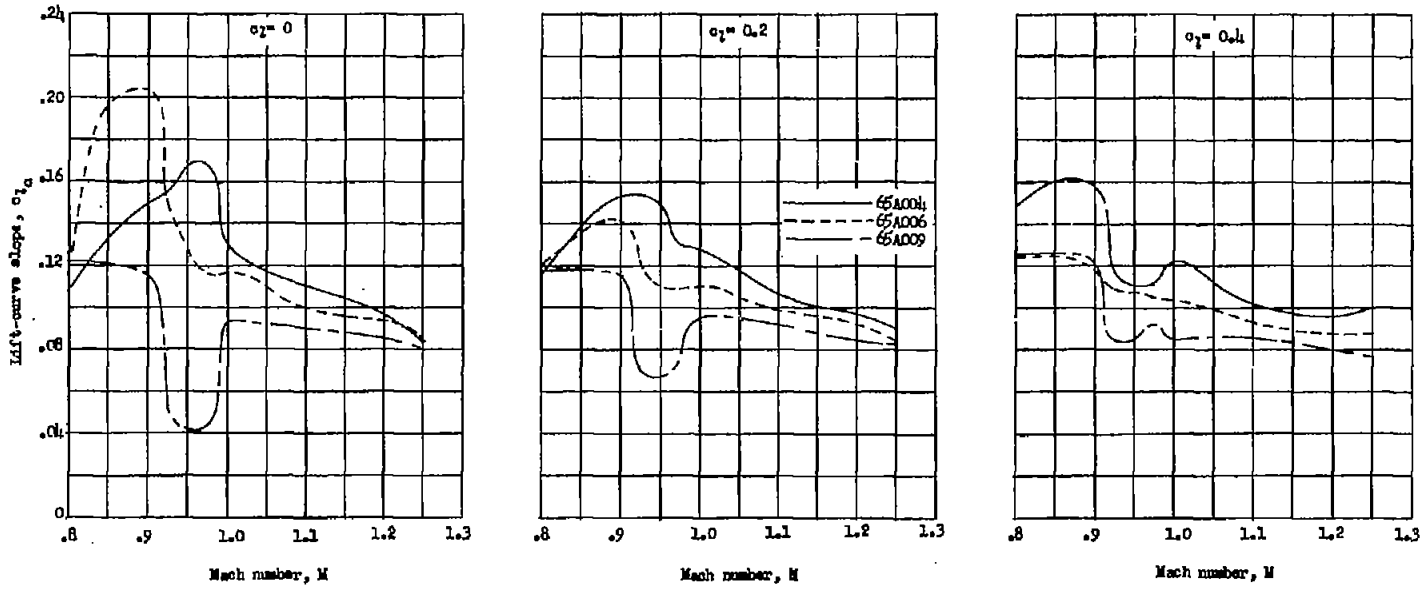

(a) Variation at several lift coefficients.

Figure 9.- Variations of section lift-curve slopes with Mach number for NACA 65A-series airfoils.

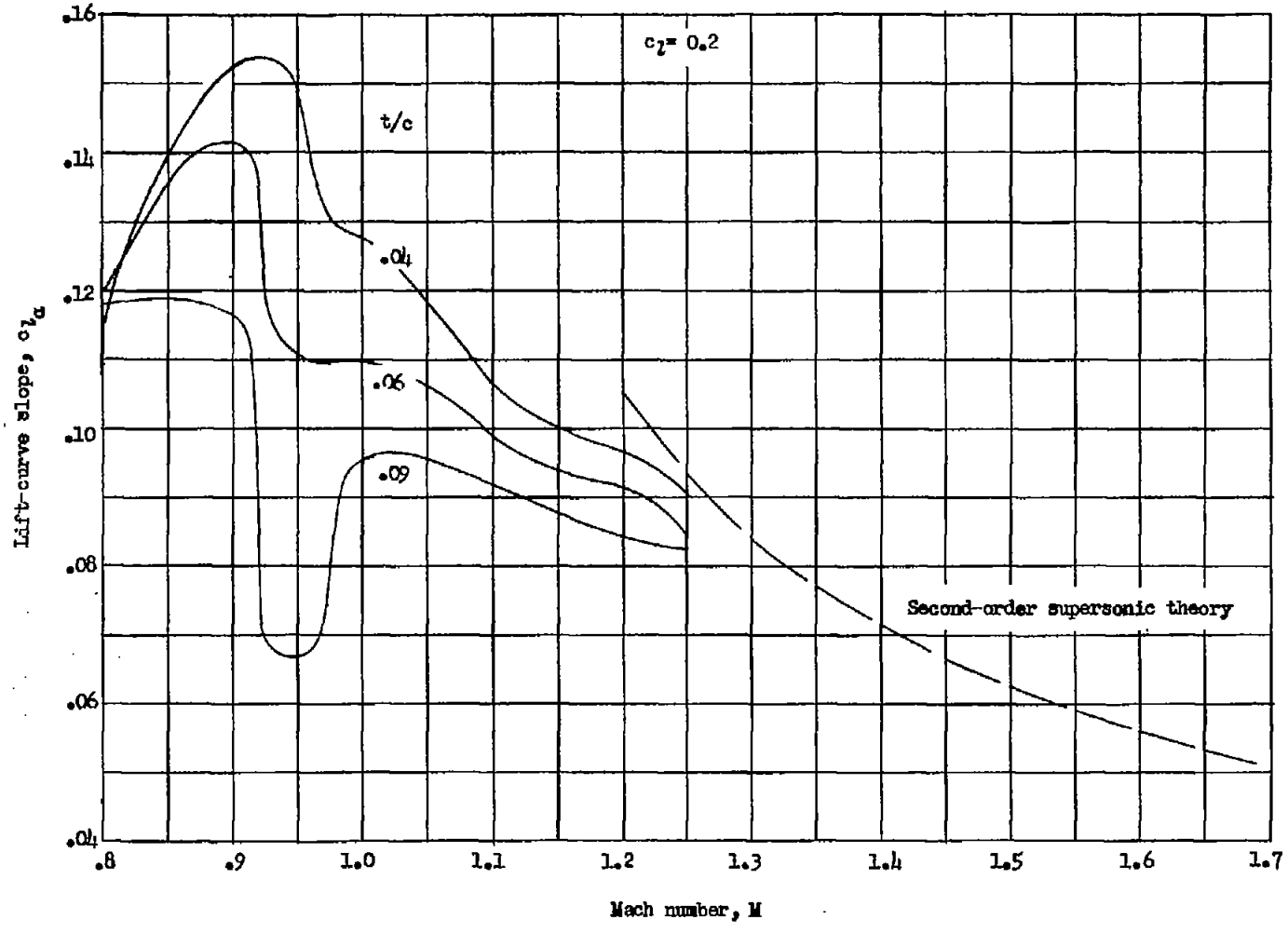

(b) Comparison with second-order supersonic theory.

Figure 9.- Concluded.

CONFIDENTIAL

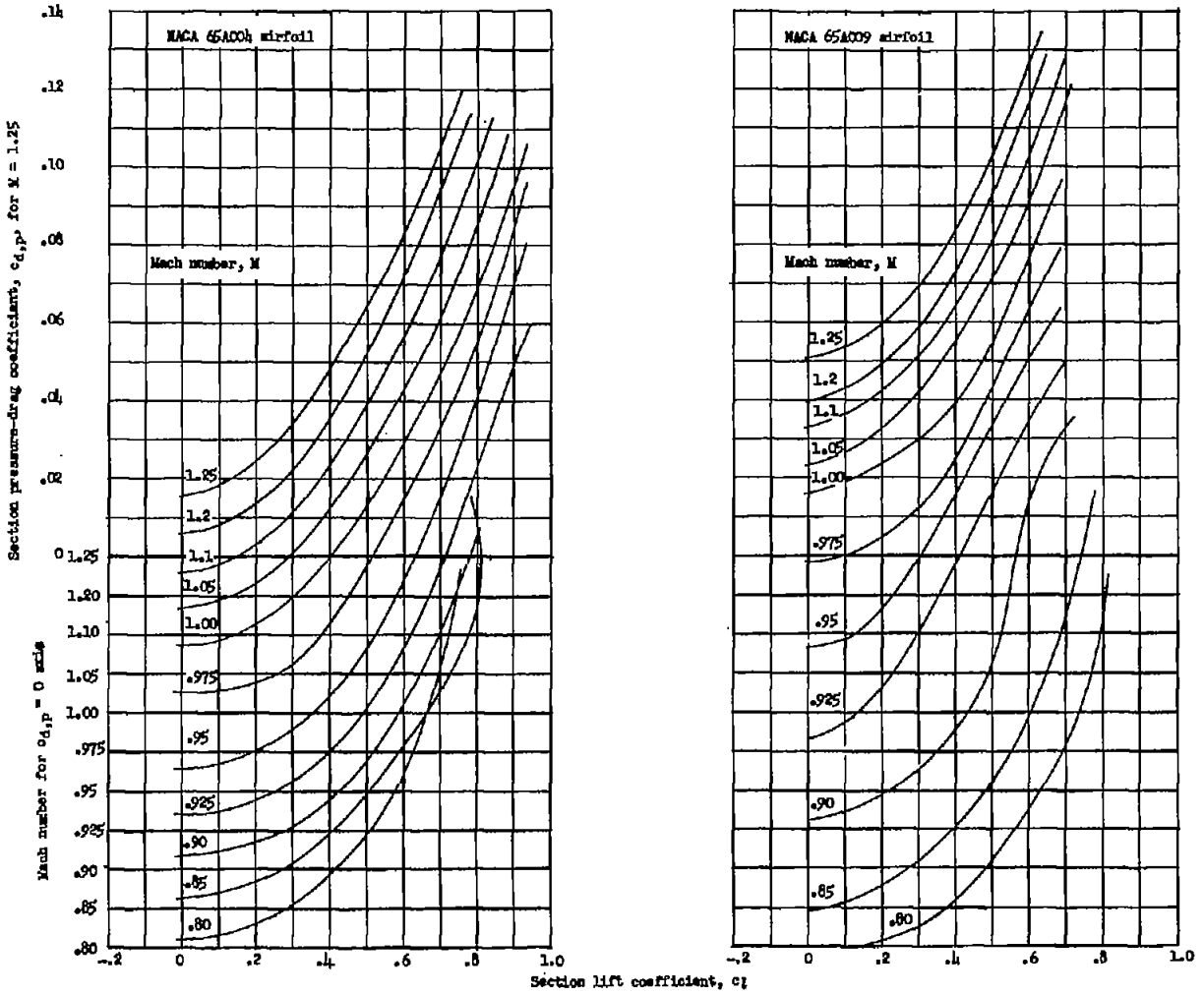

(a) NACA 65A004 and NACA 65A009 sections.

Figure 10.- Variation in section pressure-drag coefficients with lift coefficients and Mach number.

CONFIDENTIAL

CONFIDENTIAL

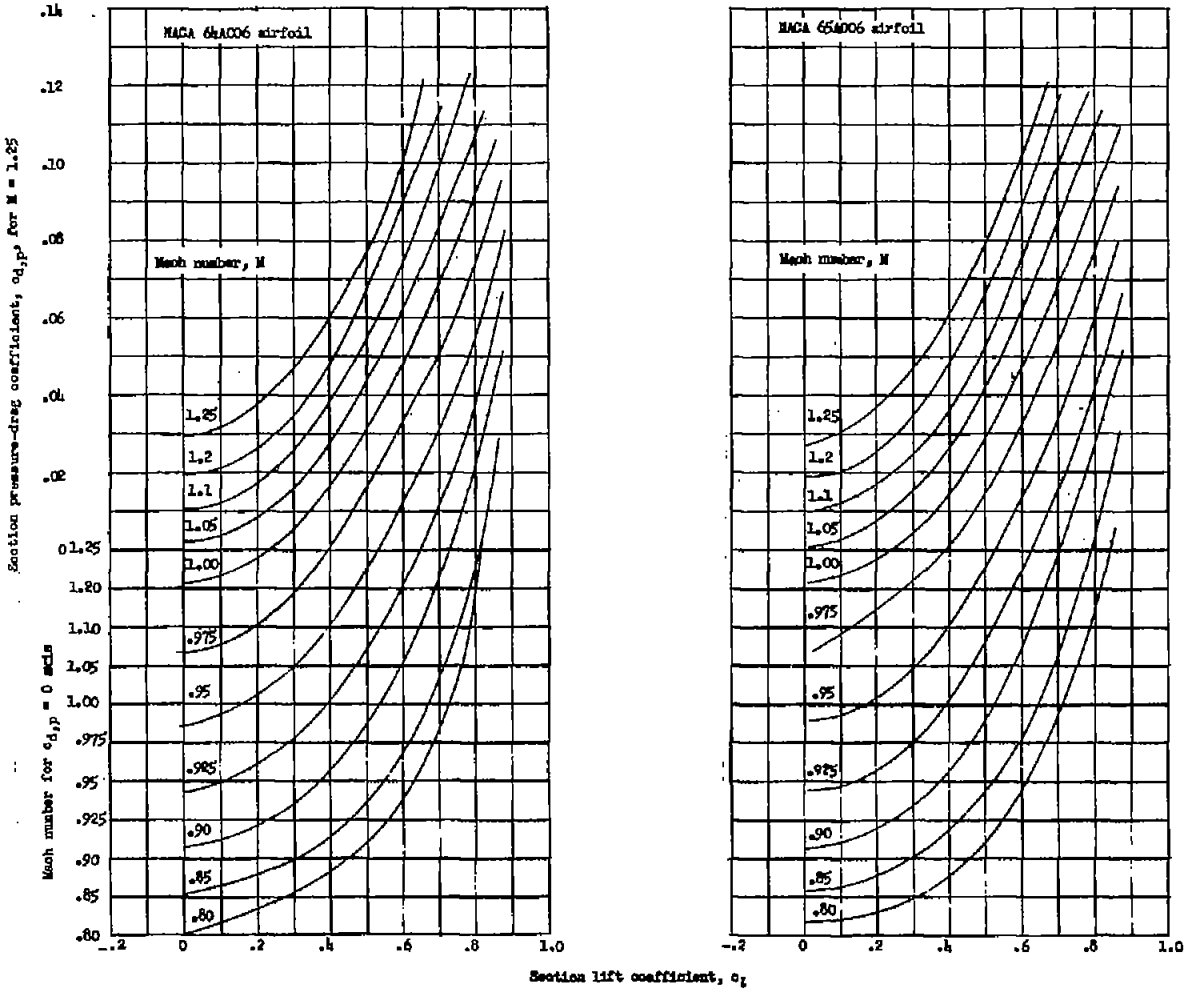

(b) NACA 65A006 and NACA 64A006 sections.

Figure 10.- Continued.

CONFIDENTIAL

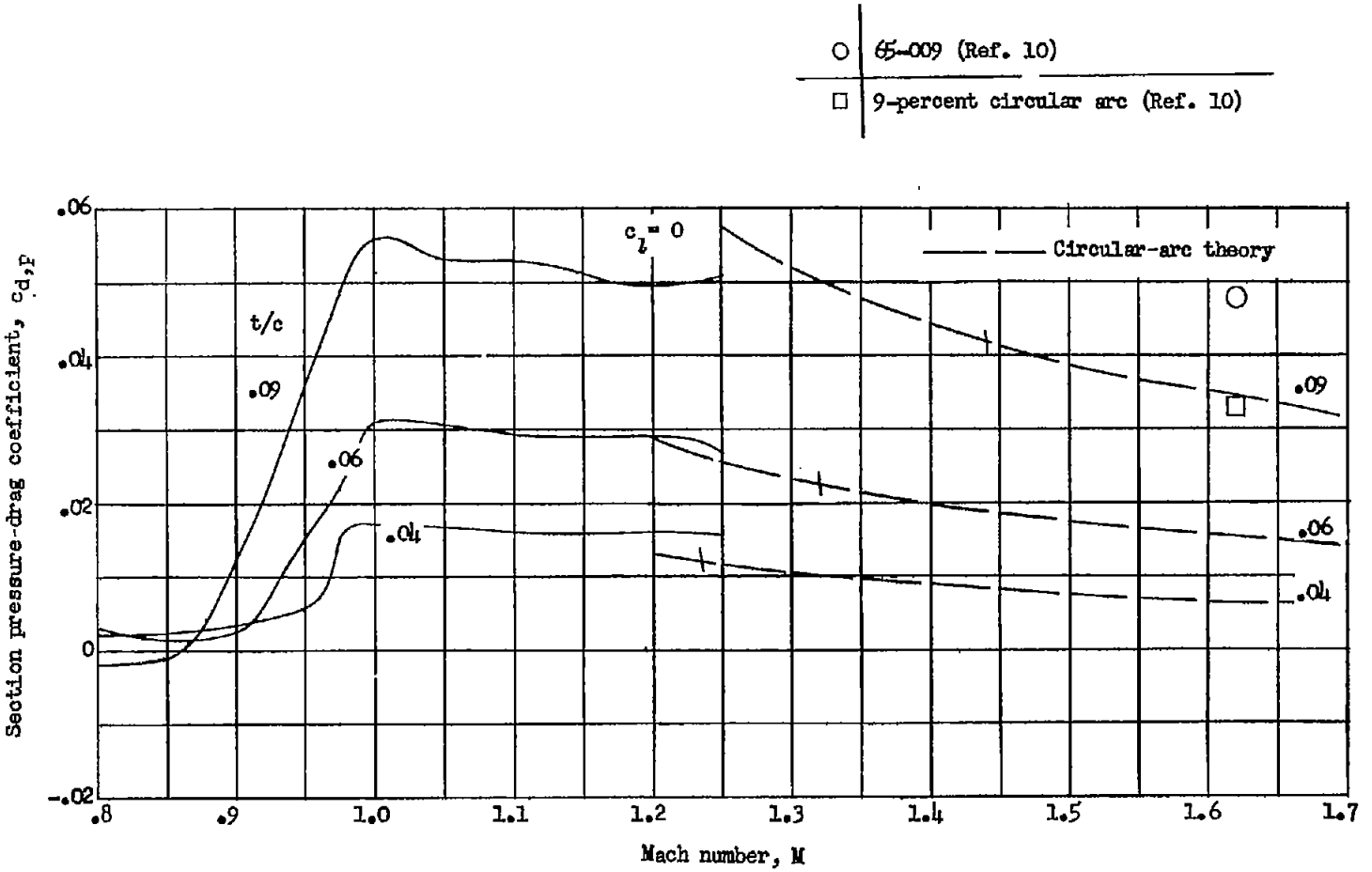

(c) Comparison with supersonic theory. $c_l = 0$.

Figure 10.- Continued.

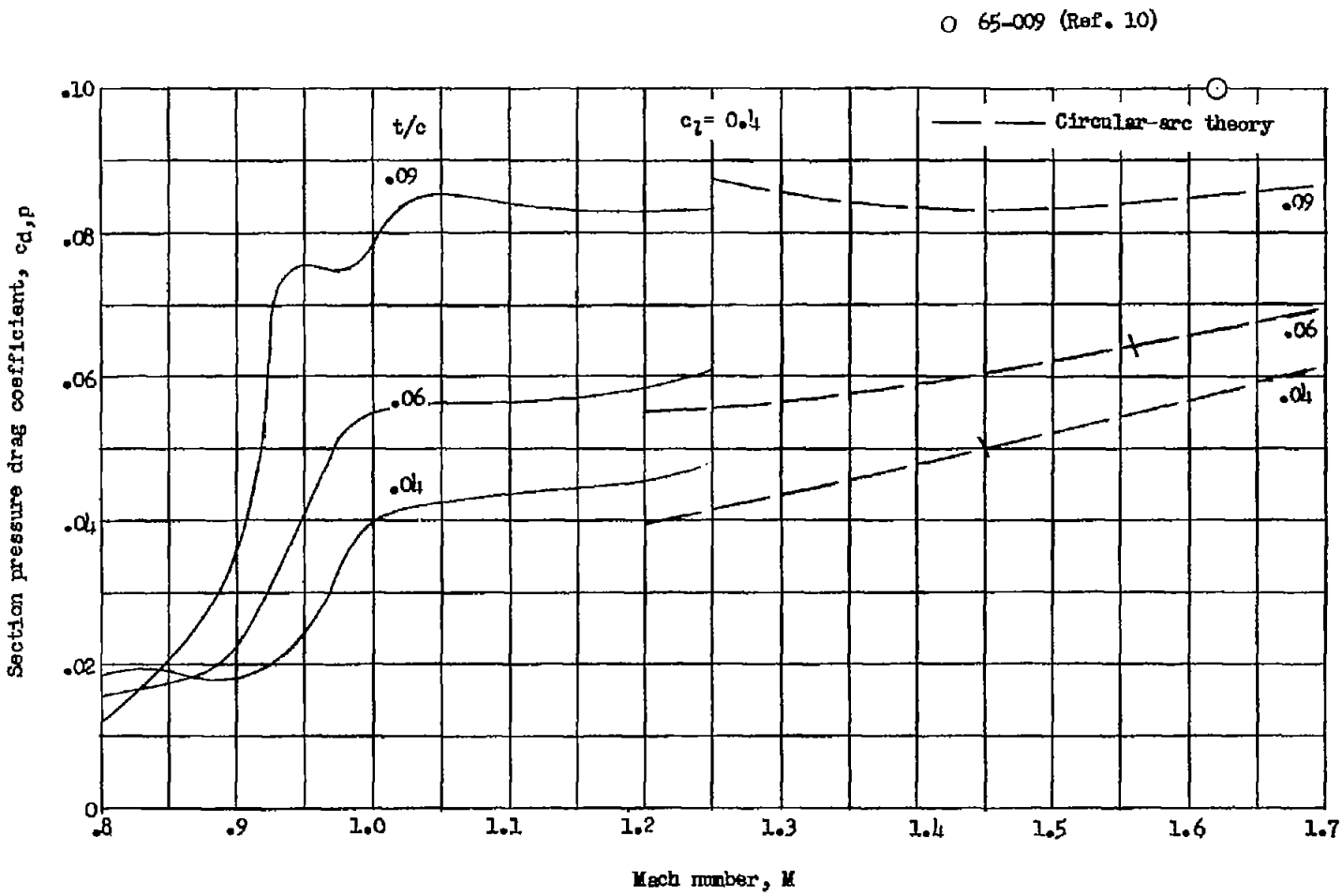

(d) Comparison with supersonic theory. $c_l = 0.4$.

Figure 10.- Concluded.

CONFIDENTIAL

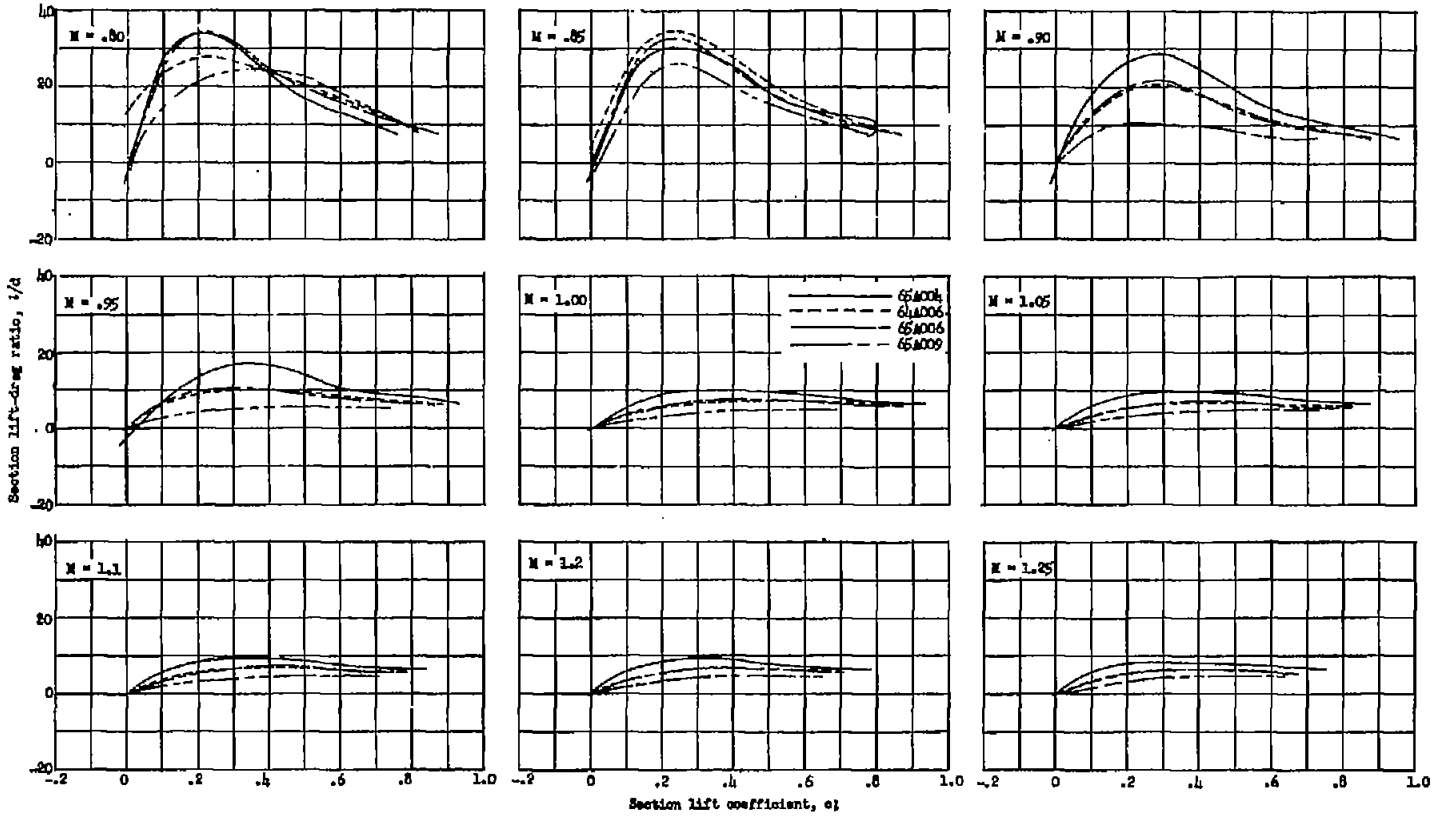

(a) Variation for various Mach numbers.

Figure 11.- Variation in section lift-drag ratios with lift coefficient and Mach number.

CONFIDENTIAL

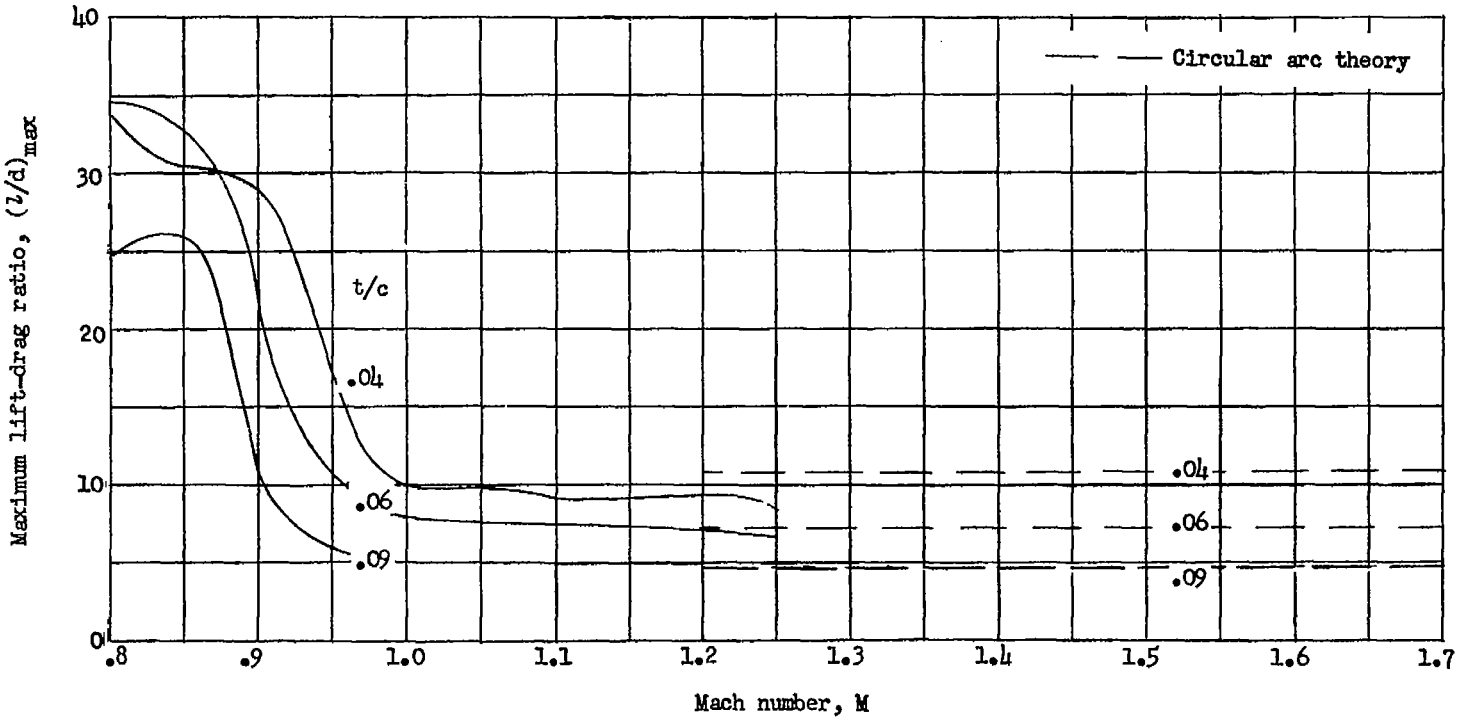

(b) Comparison of maximum lift-drag ratios with supersonic theory.

Figure 11.- Concluded.

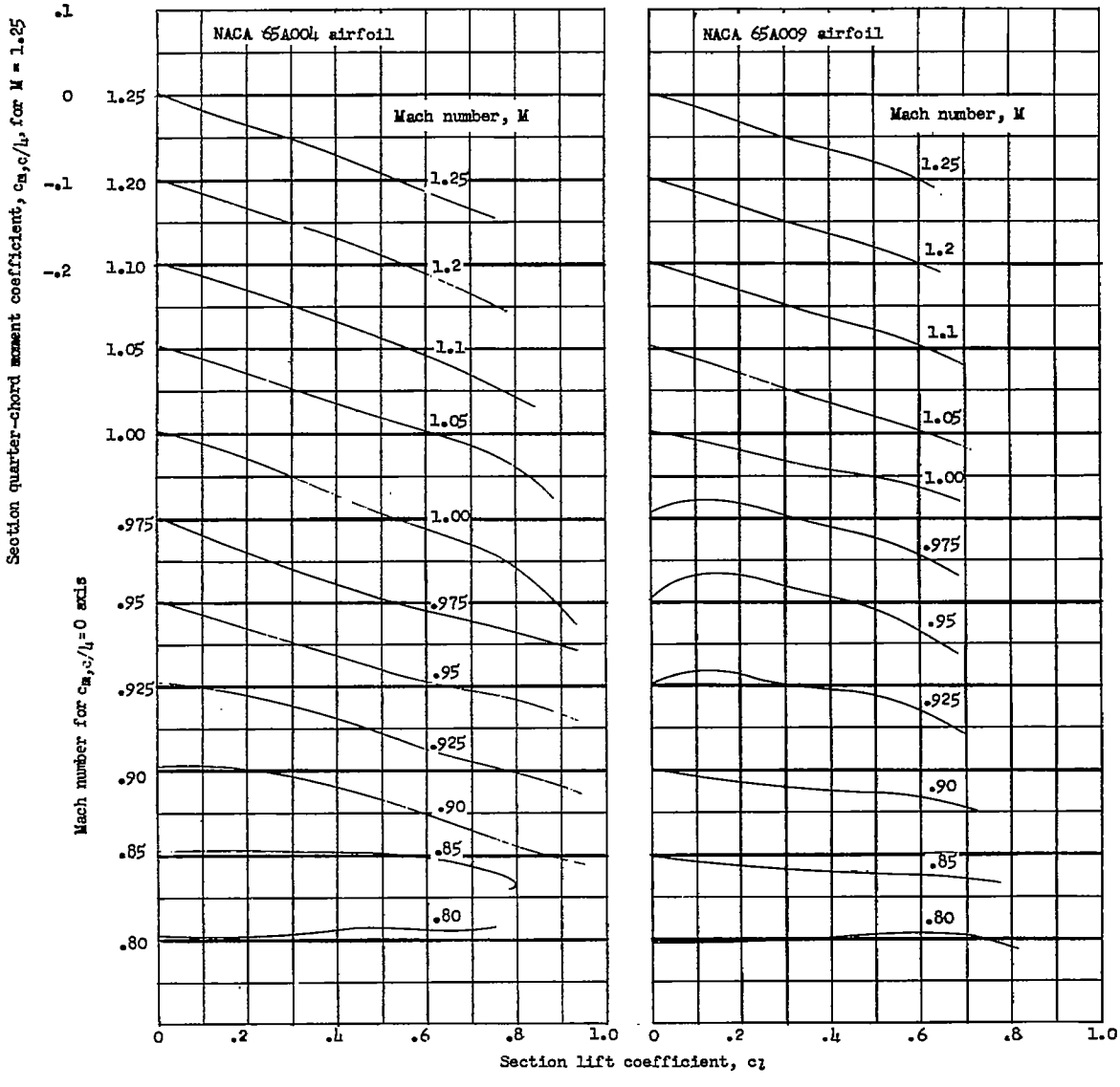

(a) NACA 65A004 and NACA 65A009 sections.

Figure 12.- Variation in section moment coefficient with Mach number and lift coefficient.

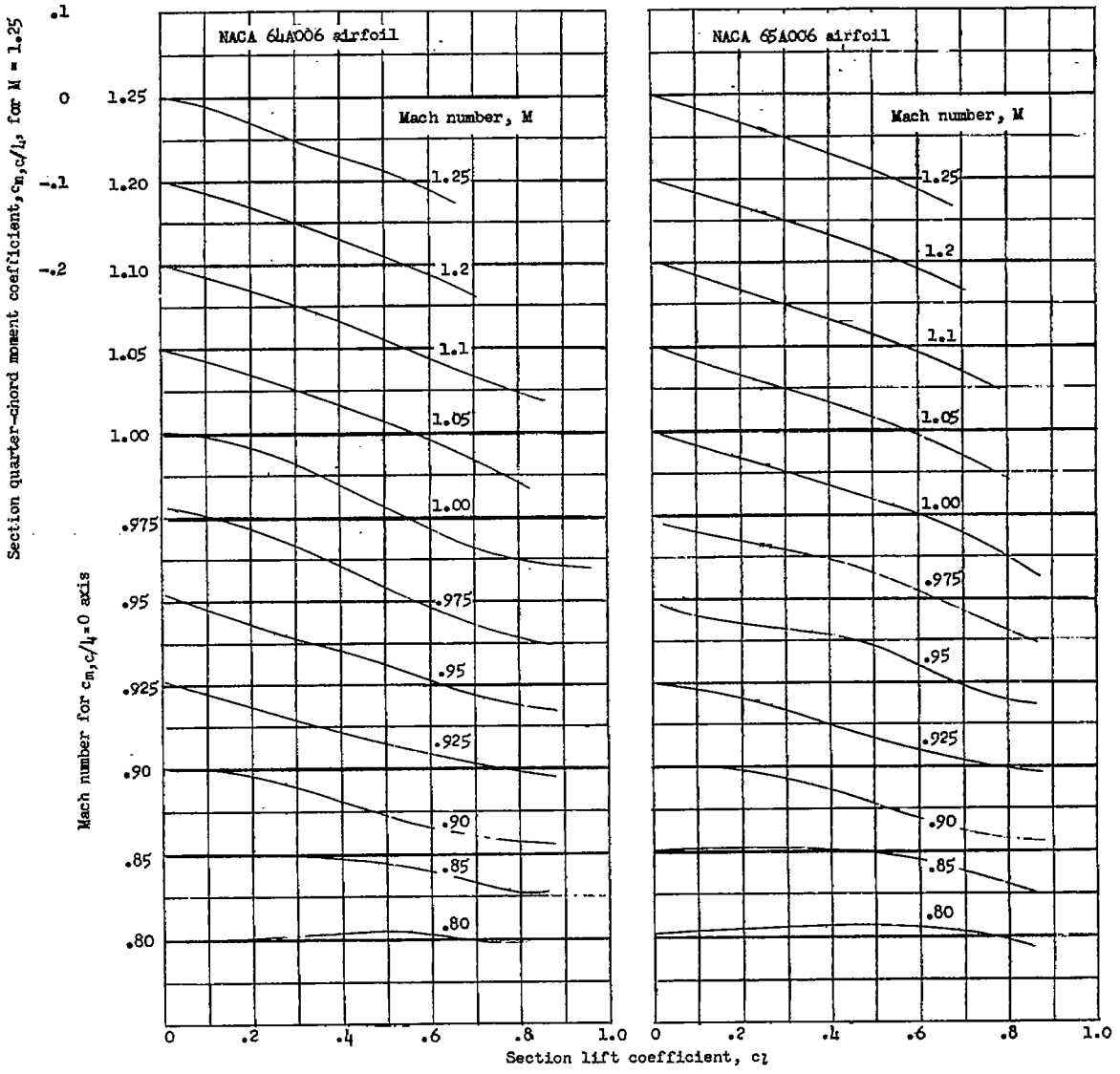

(b) NACA 65A006 and NACA 64A006 sections.

Figure 12.- Concluded.

CONFIDENTIAL

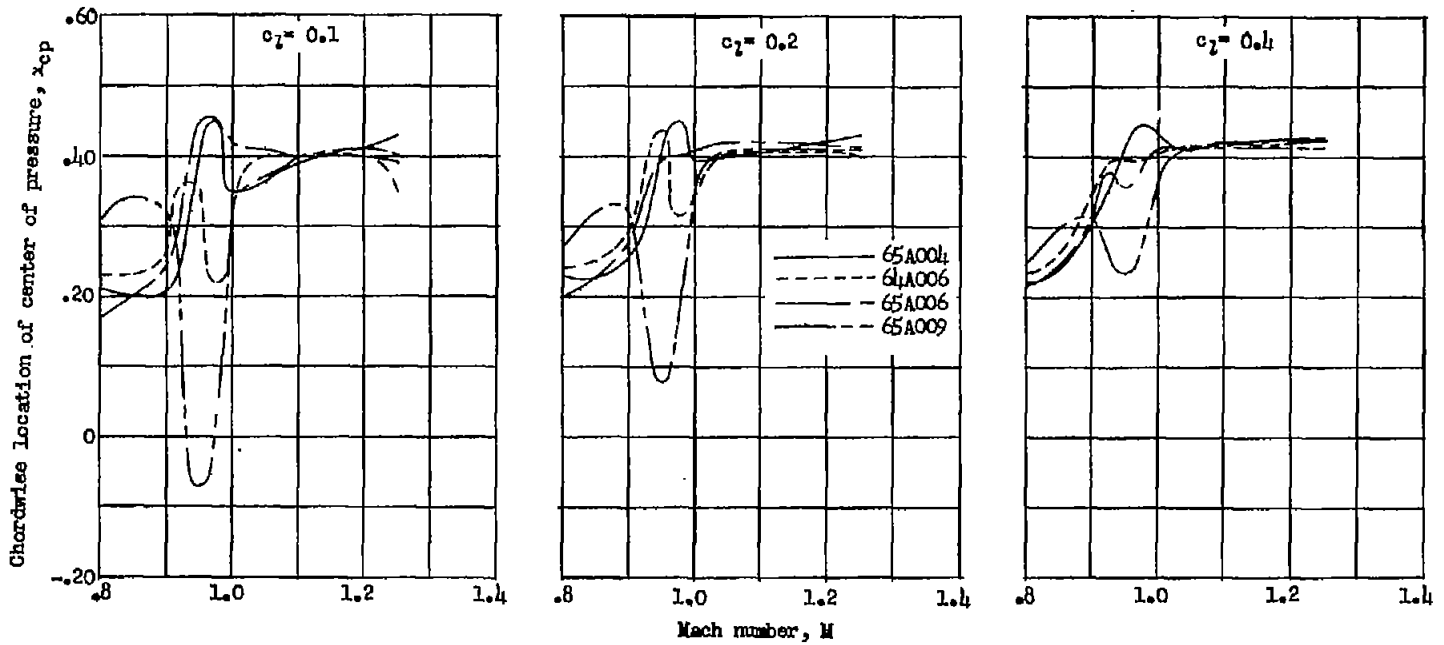

(a) Variation for various Mach numbers.

Figure 13.- Variations in location of center of pressure with Mach number and lift coefficient.

CONFIDENTIAL

CONFIDENTIAL

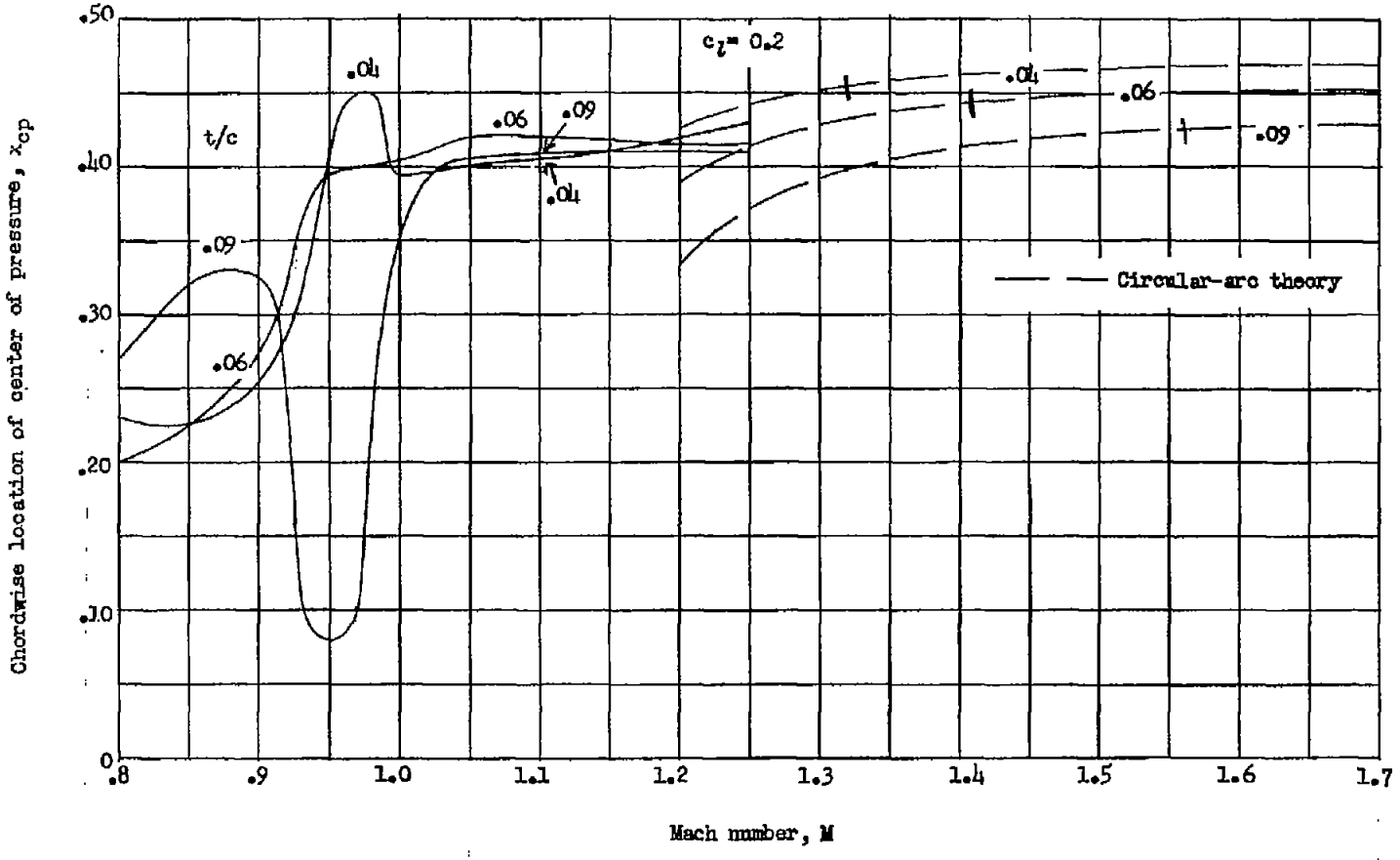

(b) Comparison with supersonic theory.

Figure 13.- Concluded.

CONFIDENTIAL

CONFIDENTIAL

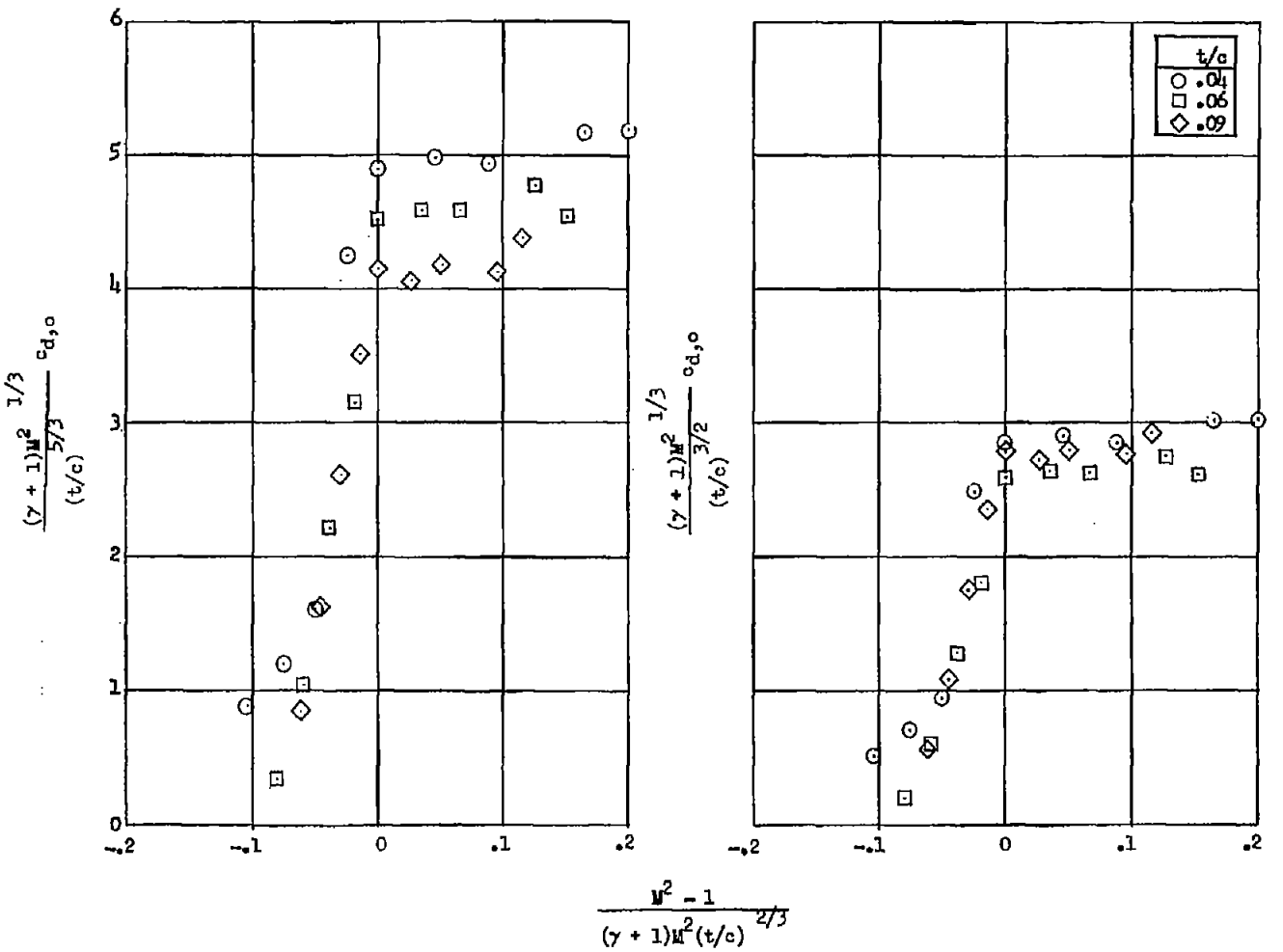

(a) Drag coefficient, unaltered form.

(b) Drag coefficient, altered form.

Figure 14.- Correlation of experimental data on NACA 65A-series airfoils by use of transonic similarity laws.

CONFIDENTIAL

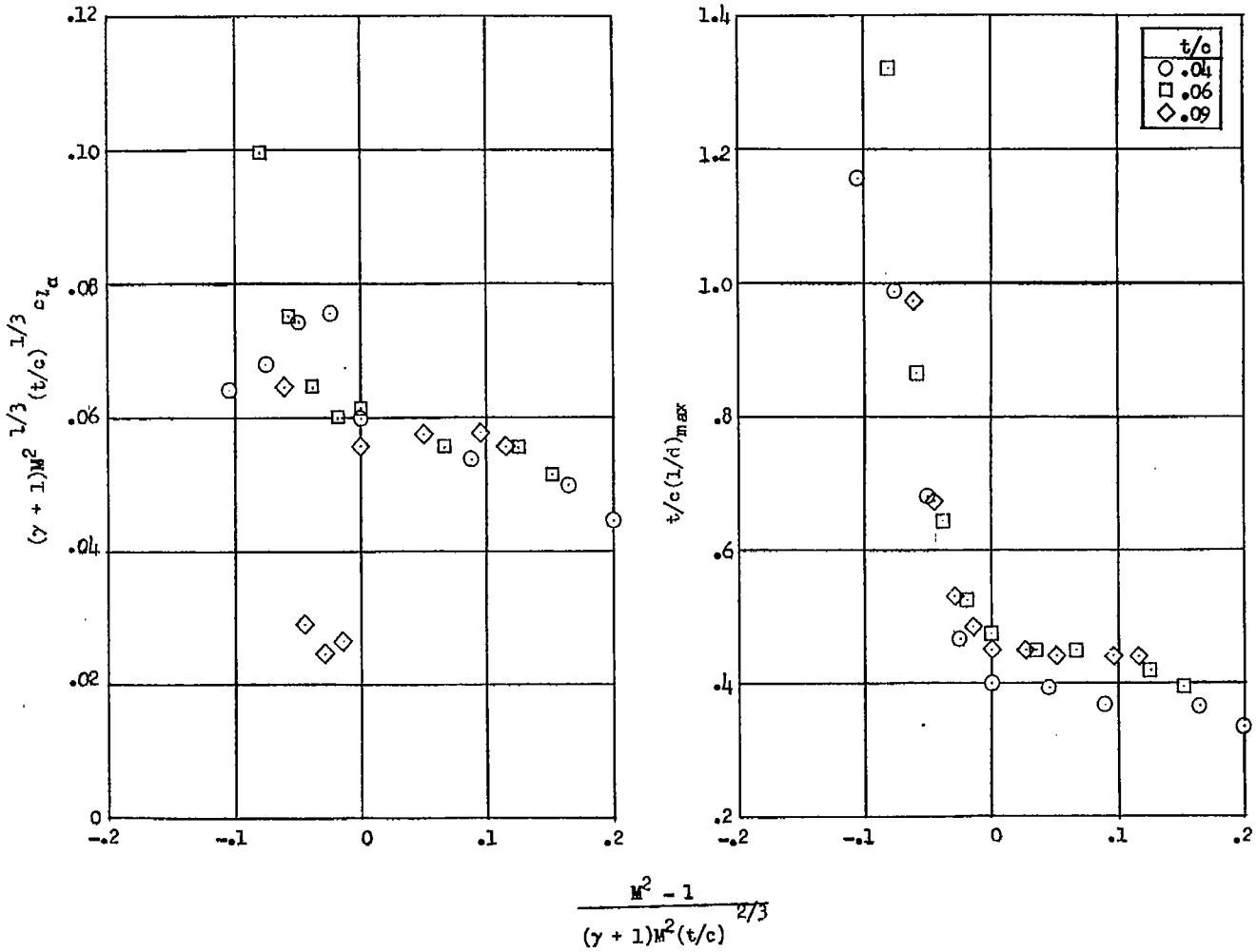

(c) Lift-curve slope.

(d) Maximum lift-drag ratios.

Figure 14.- Concluded.

CONFIDENTIAL

CONFIDENTIAL